

$\overline{\text{MS}}$ -on-shell quark mass relation up to four loops in QCD and a general $\text{SU}(N)$ gauge group

Peter Marquard,¹ Alexander V. Smirnov,² Vladimir A. Smirnov,³ Matthias Steinhauser,⁴ and David Wellmann⁴

¹*Deutsches Elektronen-Synchrotron, DESY, 15738 Zeuthen, Germany*

²*Research Computing Center, Moscow State University, 119991 Moscow, Russia*

³*Skobeltsyn Institute of Nuclear Physics of Moscow State University, 119991 Moscow, Russia*

⁴*Institut für Theoretische Teilchenphysik, Karlsruhe Institute of Technology (KIT),
76128 Karlsruhe, Germany*

(Received 21 June 2016; published 17 October 2016)

We compute the relation between heavy quark masses defined in the modified minimal subtraction and the on-shell schemes. Detailed results are presented for all coefficients of the $\text{SU}(N_c)$ color factors. The reduction of the four-loop on-shell integrals is performed for a general QCD gauge parameter. Altogether there are about 380 master integrals. Some of them are computed analytically, others with high numerical precision using Mellin-Barnes representations, and the rest numerically with the help of FIESTA. We discuss in detail the precise numerical evaluation of the four-loop master integrals. Updated relations between various short-distance masses and the $\overline{\text{MS}}$ quark mass to next-to-next-to-next-to-leading order accuracy are provided for the charm, bottom and top quarks. We discuss the dependence on the renormalization and factorization scale.

DOI: [10.1103/PhysRevD.94.074025](https://doi.org/10.1103/PhysRevD.94.074025)

I. INTRODUCTION

Quark masses are fundamental parameters of quantum chromodynamics (QCD) and thus it is mandatory to determine their numerical values as precisely as possible. Furthermore, it is important to have precise relations at hand which relate the masses in different renormalization schemes.

The renormalization scheme for the quark masses has to be fixed once quantum corrections are considered. In QCD there are two distinct renormalization schemes for the quark masses: the on-shell (OS) scheme, which is motivated by the physical interpretation of the mass parameter, and the modified minimal subtraction ($\overline{\text{MS}}$) scheme which is very convenient for many practical calculations, in particular, in high-energy processes.

In the case of the lighter quarks (up, down and strange) the meson masses are in general much larger than the masses of the quarks. Thus, the concept of the on-shell scheme is not applicable to light quark flavors; their numerical values are usually given in the $\overline{\text{MS}}$ scheme. On the other hand, the masses of the mesons involving charm and bottom quarks are essentially dominated by the quark masses. For this reason, the quantum corrections considered in this paper are mainly relevant for the three heavy quarks, charm, bottom and top.

The top quark plays a special role in this context. Due to its large width it decays before hadronization and thus can be considered as an almost free quark. As a consequence it can be expected that the on-shell value for the top quark can be determined with a relatively small uncertainty. This aspect has been studied in detail in recent papers [1,2]. It

has been shown that the on-shell top quark can be computed from the $\overline{\text{MS}}$ mass with an irreducible uncertainty of about 70 MeV [2].

There are various methods which can be used to obtain numerical values for the quark masses. Some of them determine directly the $\overline{\text{MS}}$ quark mass (see, e.g., Ref. [3]) and thus do not suffer from the inherent renormalon ambiguity. However, the highest sensitivity to the quark masses is in general obtained from physical quantities evaluated at energies close to the quark mass. In such situations it is convenient to introduce so-called threshold masses to parametrize the physical quantities. Among the most prominent ones are the potential subtracted (PS) [4], 1S [5–7], renormalon subtracted (RS) [8] and the kinetic mass [9].¹ They allow for a precise determination of the heavy $\overline{\text{MS}}$ mass without explicit reference to the pole quark mass. However, at intermediate stages the pole mass and, in particular, the relation between the pole and the $\overline{\text{MS}}$ mass is still needed.

In the following we describe three typical examples where the four-loop terms in the mass relations turn out to be important.

- (i) At the TEVATRON and the LHC the top quark mass is measured with an uncertainty below 1 GeV. For example, the combination of results from ATLAS, CDF, CMS and D0 from March 2014 [10] leads to

¹Note that the relation of the kinetic mass to the on-shell mass is currently only known to next-to-next-to-leading order (NNLO). For this reason it is not considered in the following.

$$M_t = 173.34 \pm 0.27(\text{stat}) \pm 0.71(\text{syst}) \text{ GeV}, \quad (1)$$

with a total uncertainty of 760 MeV. The value in Eq. (1) is often called ‘‘Monte-Carlo mass’’ and there are several attempts which suggest methods to relate it to the on-shell mass (see, e.g., Refs. [11–13]). In case Eq. (1) is interpreted as the on-shell quark mass it has to be converted to the $\overline{\text{MS}}$ top quark mass. Note that the three-loop term in the conversion formulas contributes approximately 500 MeV which is of the same order as the experimental uncertainties in Eq. (1).

- (ii) From measurements of the top quark pair production cross section close to threshold at a future linear collider it will be possible to determine the top quark threshold mass with an accuracy below 100 MeV (see, e.g., Refs. [14,15]). In the conversion to the $\overline{\text{MS}}$ definition there is a contribution of about 150–200 MeV from the three-loop term in the mass relations which contributes significantly to the final uncertainty of the $\overline{\text{MS}}$ mass (see Sec. IV B for precise numbers). With the help of the four-loop $\overline{\text{MS}}$ -on-shell relation this uncertainty can be drastically reduced.

For the sake of completeness let us mention that there is an approach to determine directly the $\overline{\text{MS}}$ top quark mass from the threshold cross section (see, e.g., Ref. [16]). In future it will be interesting to compare the top quark mass values obtained with different methods.

- (iii) The bottom quark mass can be extracted from Υ sum rules (see Refs. [17,18] for recent N^3LO analyses) and from $M(\Upsilon(1S))$ [19–22]. Usually, in a first step a threshold mass is obtained. To be able to compare with the $\overline{\text{MS}}$ quark mass (as, e.g., extracted from low-moment sum rules [3]) one has to apply the corresponding conversion formula. At three loops the contribution is of the order of 30 MeV, which is of the same order of magnitude (in some cases even larger) than the combination of all other uncertainties involved.

These examples show that the three-loop contribution is sizeable and a reliable estimate of the uncertainty is only obtained once the four-loop corrections are available. Furthermore, note that for the PS, 1S and RS masses one knows the relation to the pole mass to N^3LO . However, due to strong cancellations (see below) the N^3LO term cannot be used unless four-loop corrections to the $\overline{\text{MS}}$ and on-shell quark mass are available.

The remainder of the paper is organized as follows: In the next section we introduce the conversion factor between the on-shell and the $\overline{\text{MS}}$ mass and discuss the color decomposition of the four-loop term. Furthermore, we provide several technical details and discuss, in particular,

the numerical accuracy of the master integrals. Section III is devoted to the results of the $\overline{\text{MS}}$ -on-shell relation which we discuss for the physical limit, i.e. $N_c = 3$ and fixed number of massless quarks, n_f , but also for generic N_c and even for general $\text{SU}(N_c)$ color factors. Several applications of the $\overline{\text{MS}}$ -on-shell relation are discussed in Sec. IV and our conclusions are contained in Sec. V.

II. TECHNICALITIES

A. Mass relations

The relation between the bare (m_0) and renormalized mass in the $\overline{\text{MS}}$ scheme (m) is given by

$$m_0 = Z_m^{\overline{\text{MS}}} m, \quad (2)$$

where $Z_m^{\overline{\text{MS}}}$ only contains poles in ϵ . It is obtained by requiring that the renormalized propagator is finite. Note that in QCD the fermion propagator contains two Lorenz structures (scalar and vector). Thus next to $Z_m^{\overline{\text{MS}}}$ also the $\overline{\text{MS}}$ wave function renormalization constant is determined. $Z_m^{\overline{\text{MS}}}$ has been computed to five-loop order in Ref. [23]; for our calculation only four-loop corrections [24–26] are needed. We use $Z_m^{\overline{\text{MS}}}$ expressed for generic $\text{SU}(N_c)$ color factors which can be extracted from the anomalous dimension given in [25]. For convenience we present the result for $Z_m^{\overline{\text{MS}}}$ in Appendix F. Note that the $\overline{\text{MS}}$ -renormalized mass m depends on the renormalization scale μ which is suppressed in Eq. (2). $Z_m^{\overline{\text{MS}}}$ depends on μ via the strong coupling constant $\alpha_s(\mu)$.

In the on-shell renormalization scheme one requires that the quark two-point function vanishes at the position of the on-shell mass M which fixes the renormalization constant Z_m^{OS} introduced via

$$m_0 = Z_m^{\text{OS}} M. \quad (3)$$

Note that m_0 and M are μ independent and Z_m^{OS} contains $\alpha_s(\mu)$ and $\log(\mu/M)$ terms. The on-shell wave function renormalization constant is determined from the requirement that the quark propagator has a residue $-i$ at $q^2 = M^2$. This leads to a formula for Z_2^{OS} which is independent of Z_m^{OS} . This is different in the $\overline{\text{MS}}$ scheme where $Z_m^{\overline{\text{MS}}}$ and $Z_2^{\overline{\text{MS}}}$ have to be determined simultaneously.

A formula for Z_m^{OS} is conveniently derived by considering the renormalized quark propagator

$$S_F(q) = \frac{-iZ_2^{\text{OS}}}{\not{q} - m_{q,0} + \Sigma(q, M)}; \quad (4)$$

$\Sigma(q, M)$ is the (amputated) quark self energy which can be split into a scalar and vector contribution

$$\Sigma(q, M) = M\Sigma_S(q^2, M) + q\Sigma_V(q^2, M), \quad (5)$$

where Σ_S and Σ_V only depend of q^2 , the (renormalized) quark mass and μ (which is again suppressed). They are obtained from the self energy Σ with the help of the projectors

$$\Sigma_S((M^2, M) = \frac{1}{4M} \text{Tr}(\Sigma(q, M))|_{q^2=M^2}, \quad (6)$$

$$\Sigma_V((M^2, M) = \frac{1}{4q^2} \text{Tr}(q/\Sigma(q, M))|_{q^2=M^2}. \quad (7)$$

Sample Feynman diagrams contributing to $\Sigma(q, M)$ are shown in Fig. 1.

Requiring that the inverse quark propagator, $[S_F(q)]^{-1}$, vanishes at the position of the on-shell mass, i.e.

$$S_F(q) \xrightarrow{q^2 \rightarrow M^2} \frac{-i}{\not{q} - M}, \quad (8)$$

leads to

$$Z_m^{\text{OS}} = 1 + \Sigma_S(M^2, M) + \Sigma_V(M^2, M). \quad (9)$$

Thus, for the evaluation of the n -loop contribution to Z_m^{OS} n -loop on-shell integrals have to be computed.

In this paper we present results for the finite quantity

$$z_m(\mu) = \frac{m(\mu)}{M} = \frac{Z_m^{\text{OS}}}{Z_m^{\text{MS}}}, \quad (10)$$

which is obtained from Eqs. (2) and (9). Note that $z_m(\mu)$ depends on $\alpha_s(\mu)$ and $\log(\mu/M)$ and has the following perturbative expansion,

$$z_m(\mu) = \sum_{n \geq 0} \left(\frac{\alpha_s(\mu)}{\pi} \right)^n z_m^{(n)}(\mu), \quad (11)$$

with $z_m^{(0)} = 1$. For later convenience we decompose $z_m^{(n)}(\mu)$ into

$$z_m^{(n)}(\mu) = z_m^{(n)}(M) + z_m^{(n), \log}, \quad (12)$$

where the second term on the right-hand side comprises the μ -dependent terms which vanish for $\mu = M$. Analytic results for $z_m^{(n), \log}$ are given in Appendix C.

For later use we also introduce the inverted relation to Eq. (10),

$$c_m(\mu) = \frac{M}{m(\mu)}, \quad (13)$$

with

$$c_m(\mu) = \sum_{n \geq 0} \left(\frac{\alpha_s(\mu)}{\pi} \right)^n c_m^{(n)}(\mu), \quad (14)$$

and $c_m^{(0)} = 1$. $c_m^{(n)}(\mu)$ is a function of $\log(\mu/m(\mu))$. Furthermore, we assume the similar decomposition of Eq. (12) with $c_m^{(n), \log} = 0$ for $\mu = m(m)$.

In this paper we consider generic $SU(N_c)$ color factors and present results for the coefficients. The four-loop term of Eq. (11) can be decomposed into 23 color structures which are given by

$$\begin{aligned} z_m^{(4)} = & C_F^4 z_m^{FFFF} + C_F^3 C_A z_m^{FFFA} + C_F^2 C_A^2 z_m^{FFAA} + C_F C_A^3 z_m^{FAAA} + \frac{d_F^{abcd} d_A^{abcd}}{N_c} z_m^{d_{FA}} + n_l \frac{d_F^{abcd} d_F^{abcd}}{N_c} z_m^{d_{FFL}} + n_h \frac{d_F^{abcd} d_F^{abcd}}{N_c} z_m^{d_{FFH}} \\ & + C_F^3 T n_l z_m^{FFFL} + C_F^2 C_A T n_l z_m^{FFAL} + C_F C_A^2 T n_l z_m^{FAAL} + C_F^2 T^2 n_l^2 z_m^{FFLL} + C_F C_A T^2 n_l^2 z_m^{FALL} + C_F T^3 n_l^3 z_m^{FLLL} \\ & + C_F^3 T n_h z_m^{FFFH} + C_F^2 C_A T n_h z_m^{FFAH} + C_F C_A^2 T n_h z_m^{FAAH} + C_F^2 T^2 n_h^2 z_m^{FFHH} + C_F C_A T^2 n_h^2 z_m^{FAHH} + C_F T^3 n_h^3 z_m^{FHHH} \\ & + C_F^2 T^2 n_l n_h z_m^{FFLH} + C_F C_A T^2 n_l n_h z_m^{FALH} + C_F T^3 n_l^2 n_h z_m^{FLLH} + C_F T^3 n_l n_h^2 z_m^{FLHH}, \end{aligned} \quad (15)$$

where C_F and C_A are the eigenvalues of the quadratic Casimir operators of the fundamental and adjoint representation for the $SU(N_c)$ color group, respectively, $T = 1/2$ is the index of the fundamental representation, and n_l and n_h count the number of massless and massive (with mass M) quarks. In the applications discussed in Sec. IV we use $n_h = 1$. It is nevertheless convenient to keep the variable n_h as a parameter. d_F^{abcd} and d_A^{abcd} are the symmetrized traces of four generators in the fundamental and adjoint representation, respectively. The color structures in Eq. (15) are related to N_c via² (see, e.g., Ref. [27])

$$C_F = \frac{N_c^2 - 1}{2N_c}, \quad C_A = N_c, \quad T = \frac{1}{2}, \quad d_F^{abcd} d_F^{abcd} = \frac{(N_c^2 - 1)(N_c^4 - 6N_c^2 + 18)}{96N_c^2}, \quad d_F^{abcd} d_A^{abcd} = \frac{N_c(N_c^2 - 1)(N_c^2 + 6)}{48}. \quad (16)$$

In the case of QCD we have $N_c = 3$.

²Note that our results are also valid for other groups. The corresponding expressions can easily be obtained by the proper choice of the group theory factors; see, e.g., Ref. [27]. We restrict ourselves to $SU(N_c)$ since it is closely connected to QCD.

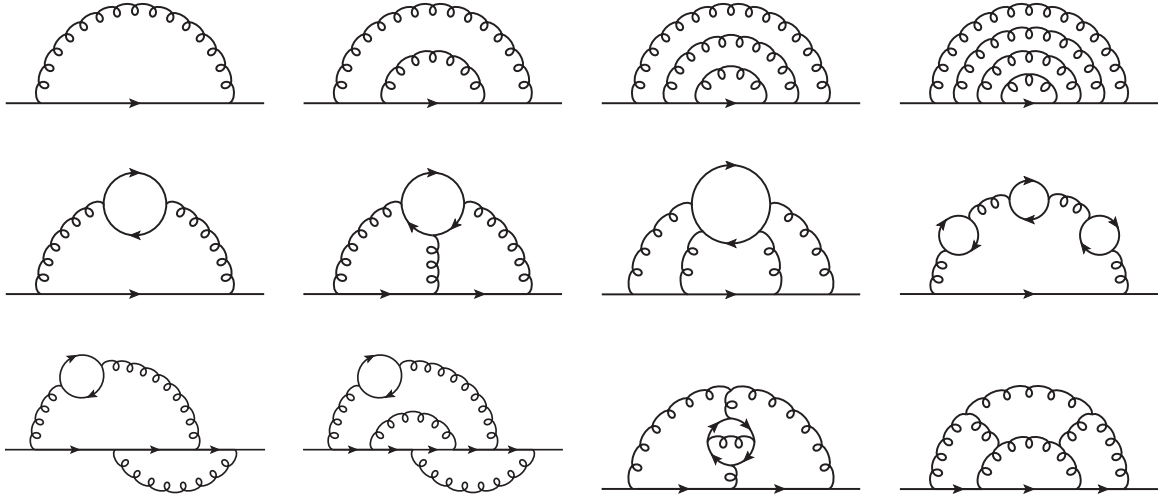


FIG. 1. Sample Feynman diagrams contributing to Σ_S and Σ_V at one-, two-, three- and four-loop order. The solid lines represent quarks and the curly lines gluons.

One-, two- and three-loop QCD results to Z_m^{OS} have been computed in Refs. [28,29] and [30–33], respectively, and electroweak effects have been considered in Refs. [34–43]. In Ref. [44] the four-loop results for z_m have been presented for $N_c = 3$ and $n_l = 3, 4$ and 5 with a numerical precision of 3% in the four-loop coefficient evaluated at $\mu = M$. It is the aim of the present paper to generalize the findings of [44] to general N_c and arbitrary n_l . Furthermore, the precision is significantly improved. In this paper we do not study light-quark mass effects which are known at two [29] and three loops [45].

The relations between the threshold and the \overline{MS} masses are too long so that we refrain from printing them in explicit form. For practical purposes it is convenient to use their implementation in `RunDec` [46] and `CRunDec` [47]. The construction of the relations can be found in the original literature [4–8]; a summary can be found in, e.g., Ref. [44].

B. Reduction to master integrals

For the calculation of Σ_S and Σ_V we use a highly automated and well-established setup based on

`qgraf` [48], `q2e` and `exp` [49,50] and in-house *Mathematica* and `FORM` [51,52] programs which work hand in hand to minimize the manual interaction. Color factors are computed with the help of `color` [27].

We use `qgraf` for the generation of the 3100 fermion self-energy amplitudes. They are converted to `FORM` code using `q2e` and `exp`. A further task of the program `exp` is to map each diagram to one out of a set of 102 predefined integral families which are shown in graphical form in Appendix A. To obtain these families we start with the 11 prototypes shown in Fig. 2. They serve as the basis to generate the allowed families by considering all possible routings of a massive line through the diagrams. Diagrams with self-energy insertions can be obtained from the ones in Fig. 2 by removing some lines and raising the propagator powers of other lines. For convenience we show a pictorial representation for each family in Appendix A. At four loops, they are labeled by 14 indices that correspond to powers of propagators and irreducible numerators. The maximal number of positive indices is 11.

We use in-house `FORM` programs to apply the projectors to the vector and scalar parts of the fermion propagator

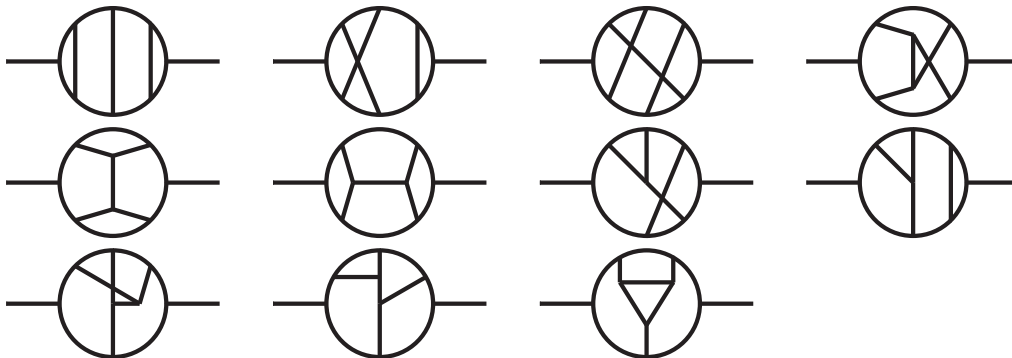


FIG. 2. Four-loop prototype families needed to generate the four-loop on-shell integral families shown in Appendix A.

needed for the calculation of the on-shell quark mass, to perform traces and to decompose the scalar products in the numerator in terms of denominator factors. As an outcome our result is written as a linear combination of scalar Feynman integrals which are related by integration-by-parts identities [53]. We apply to each family the Laporta algorithm [54] as implemented in FIRE [55–57] and Crusher [58] to perform a reduction to master integrals.

We first work with each of the individual families and determine the corresponding master integrals. It turns out that the primary sets of the master integrals revealed with FIRE are not minimal, i.e. there exist additional relations among them. Then, following Ref. [56], we find additional relations using symmetries of various integrals with indices 0, 1, and 2. For each sector³ one can estimate the number of the master integrals using the code Mint [59]. There are, however, additional relations which connect master integrals of partially overlapping sectors and they can be revealed by the same procedure based on symmetries. The number of the master integrals in a given family can be as large as 176.

One more criterion when looking for additional relations is the absence of a spurious dependence of denominators in reduction relations on d . The general analysis of singularities of Feynman integrals as functions of d shows that poles in d can be only real rational numbers. So, if we observe a nonfactorizable polynomial of second or higher degree in d in a denominator this means that either we miss a relation between the current master integrals or some master integrals are chosen in an inappropriate way. At least in all the cases in our calculation, we managed to get rid of such spurious denominators by revealing additional relations or making better choices of the master integrals. However, with the sets of master integrals we have arrived at it is not guaranteed that we have really minimal sets of master integrals, i.e. bases of the corresponding linear spaces.

The next step was to find relations between master integrals of various families. To do this, we used the *Mathematica* code `tsort` which is part of the latest FIRE version [57] and end up with 386 four-loop massive on-shell propagator integrals, i.e. with $q^2 = M^2$.

We have performed the calculation allowing for a general gauge parameter ξ keeping terms up to order ξ^2 in the expression we give to the reduction routines. We have checked that ξ drops out after adding counterterm contributions from mass renormalization which is a welcome cross-check on the consistency of our result.

As was mentioned above the algorithms we use to minimize the number of basis integrals does not guarantee that we obtain all relations among the integrals which appear as master integrals of the individual families. The fact that ξ drops out before using explicit results for the

³A sector is a subset of indices where some indices are positive and the other indices are nonpositive.

master integrals is a hint that we are at least close to the minimal set.

We refrain from listing all master integrals but provide some examples in the next subsection where the numerical accuracy of those integrals is discussed which cannot be computed analytically.

Let us stress that up to this point our calculation is completely analytical.

C. Computation of master integrals

In this subsection we describe the methods that have been used to obtain results for the master integrals.

All master integrals are computed numerically with the help of FIESTA [60–62]. FIESTA applies the sector decomposition algorithm which leads to a, in general, multidimensional integral representation of the coefficients of the ϵ expansion. The integration is performed using Monte Carlo methods as implemented in the CUBA [63] library. FIESTA allows for a highly parallel numerical integration and provides an almost linear scaling behavior. In fact, most of our calculations are performed at the High Performance Computing Center Stuttgart (HLRS) and the Supercomputing Center of Lomonosov Moscow State University which provide up to 1024 CPU cores or 64 Tesla GPUs for a single run. The integral data base obtained with FIESTA provides the reference for the improvements for some of the integrals discussed in the following.

We have computed all integrals using different statistics ranging from $N = 0.5 \times 10^6$ to $N = 2 \times 10^9$ sampling points. We have observed that the uncertainty decreases proportional to $1/\sqrt{N}$ according to the expectations for Monte Carlo integrations. In Fig. 3 we show three typical master integrals which are shown in graphical form to the left of the plot. For each term of the ϵ expansion, which is indicated on the x axis, several data points are shown which correspond to different numbers of sampling points.⁴ The central values are normalized to the most precise result and then we subtract 1 which explains why the central value of the leftmost data point is equal to 0. The uncertainty bars correspond to the results where the Monte Carlo uncertainty based on Vegas [64] is multiplied by a factor 10 (see also discussion below).

For the first two examples we observe that the central values of the more precise calculation lie within the uncertainties of the less precise ones. At the same time the uncertainty is significantly reduced.⁵ The third example behaves differently: For the ϵ^1 and ϵ^2 terms we

⁴For better readability the results for different sampling points are slightly displaced.

⁵In those cases where the uncertainty does not become smaller after increasing the sampling points the requested precision is already reached for a smaller number of sampling points.

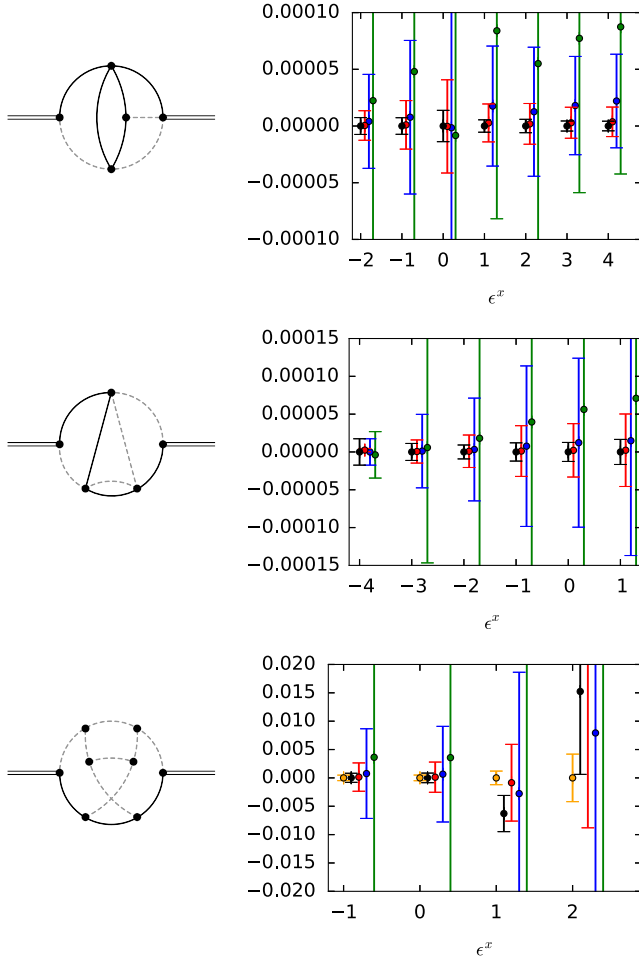


FIG. 3. FIESTA results for three typical integrals for various choices of N . The corresponding master integrals are shown to the left of the plots (see caption of Fig. 4 for the meaning of the lines). In this plot the FIESTA uncertainties have been multiplied by a factor 10. For each ϵ coefficient on the x axis results for different numbers of sampling points, N , are shown. For all plots we show results for $N = 5 \times 10^k$ with $k = 5, 6, 7, 8$. The bottom plot also contains results for $N = 2 \times 10^9$. In each case we normalize the results to the most precise one and then subtract 1.

observe relatively big jumps after increasing the sampling points from $N = 5 \times 10^7$ to $N = 5 \times 10^8$ and then to $N = 2 \times 10^9$. Furthermore, the more precise central value lies partly outside the ten-sigma uncertainty bands.

We have produced convergence plots as those in Fig. 3 for all master integrals computed with FIESTA. Note that the one in the bottom panel of Fig. 3 is among the integrals with the worst behavior. Altogether for about five master integrals the five-sigma uncertainty band is not sufficient to find agreement between the central values of the high-precision results with the uncertainty band of the low-precision results. For this reason we adopt a conservative

attitude and multiply the Monte Carlo uncertainty of FIESTA by a factor 10. The reason for such a multiplication can also be justified by the fact that each master integral leads to thousands of individual sector integrals, and each of them produces some error estimate. FIESTA uses the mean-square norm when adding up error estimates, but in unlucky situations this might be not enough for a real error estimate.

It turns out that some of the master integrals determined with FIRE, which have usually indices equal to 1 and 0, are not optimal for the subsequent numerical evaluation with FIESTA and only a poor numerical precision is obtained. In such situations, we tried to make a better choice of the master integrals replacing master integrals of some sector by other integrals which can have indices equal to 2. In some cases, we successfully followed the strategy advocated in Ref. [65] where the goal was to choose a finite or a quasifinite (in the sense that the only divergence comes from the overall gamma function in Feynman parametrization) basis.

In particular, for our final result we replaced the integral shown in the bottom panel of Fig. 3 by an integral with numerators which shows a much better convergence behavior. Let us, however, stress that the final results (discussed in the next section) for the two different bases are consistent within the uncertainties.

For all factorizable integrals, we obtained analytic results from the known one-, two- and three-loop results. In particular, we use the results of Ref. [66] where all three-loop master integrals have been obtained in an ϵ expansion up to the order typical to four-loop calculations. For four of them, G43, G53, G62, and G65 (see Fig. 3 of [66]) we had to add an additional order in ϵ which is straightforward. In most cases one can derive a one-dimensional Mellin-Barnes representation which converges exponentially and thus $\mathcal{O}(1000)$ digits can easily be obtained. In our calculation we encounter in total seven factorizable integrals.

For some master integrals, analytic results could be derived using a straightforward loop-by-loop integration at general d ; see, e.g., Fig. 5 (top, leftmost). We also used analytical results obtained for the 13 nontrivial four-loop on-shell master integrals computed in our earlier paper [67] (see Figs. 3 and 4 of [67]).

At this point we adopt a practical attitude and generate an ordered list which contains the ϵ coefficients of master integrals with large contributions to the final uncertainty. This list is used as a starting point to improve the accuracy of our result by increasing the numerical precision of the corresponding master integral. Up to a certain point this could be reached by simply increasing the statistics in the approach based on FIESTA. Of course, this approach is quite limited since an increase of the number of sampling points by 10 leads to an uncertainty which is reduced by about a factor 3.

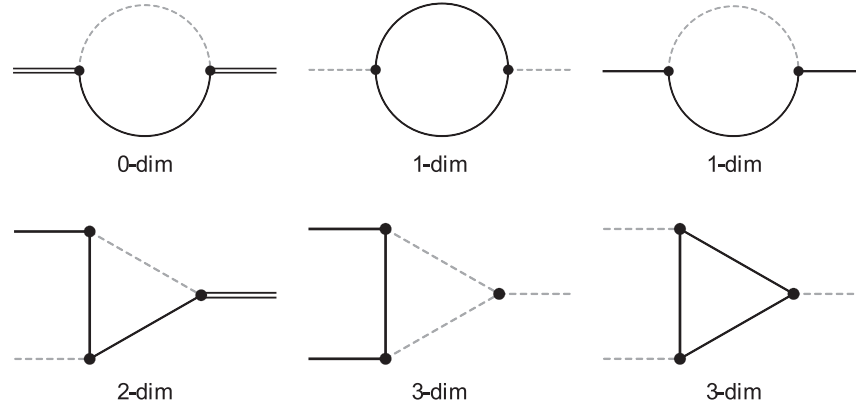


FIG. 4. Sample building blocks for the loop-by-loop approach with three different types of external legs: dashed or solid lines denote massless or massive propagators of general momentum p^2 , respectively. Their general complex powers can depend on the dimensional regularization parameter ϵ and Mellin-Barnes integration variable z_i . Double lines are on shell with the condition $p^2 = m^2$. The dimension of the Mellin-Barnes integration is specified below the diagrams.

A closer look at the generated list shows that the major contribution to the uncertainty comes from master integrals containing two- or three-point subdiagrams. For these integrals we proceed as follows:

- (i) Derive Mellin-Barnes representations for the subdiagrams.

This is achieved with the help of the formula

$$\frac{1}{(X + Y)^\lambda} = \frac{1}{\Gamma(\lambda)} \frac{1}{2\pi i} \int_{-i\infty}^{+i\infty} dz \frac{Y^z}{X^{\lambda+z}} \Gamma(\lambda + z) \Gamma(-z), \quad (17)$$

which is used to split sums in the denominator raised to arbitrary power into products. In this way massive propagators can be transformed into

massless ones at the cost of a Mellin-Barnes integration. It is worth mentioning that it does not need any specific hierarchy among the summands. Depending on the other lines of the original diagram we use the Mellin-Barnes method such that the external momenta of the subdiagram are either massive or massless. If possible, we apply on-shell conditions for external momenta.

As an example we present our results for two typical “building blocks.”

The bubble integral with two massive lines (see Fig. 4, second diagram of the first row) and with massless external legs can be written in the following form:

$$\int \frac{d^d k}{i\pi^{\frac{d}{2}}} \frac{1}{[m^2 - k^2]^{a_1} [m^2 - (k + p)^2]^{a_2}} = \frac{1}{2\pi i} \int_{-i\infty}^{+i\infty} dz \frac{(m^2)^{\frac{d}{2} - a_1 - a_2 - z} \Gamma(-z) \Gamma(a_1 + z) \Gamma(a_2 + z) \Gamma(a_1 + a_2 - \frac{d}{2} + z)}{(-p^2)^{-z} \Gamma(a_1) \Gamma(a_2) \Gamma(a_1 + a_2 + 2z)}. \quad (18)$$

The triangle integral with two massive internal lines and one massive, one massless and one on-shell leg (see first diagram of the second row in Fig. 4) is given by

$$\begin{aligned} & \int \frac{d^d k}{i\pi^{\frac{d}{2}}} \frac{1}{[m^2 - (k + p_1)^2]^{a_1} [m^2 - (k + p_1 + p_2)^2]^{a_2} [-k^2]^{a_3}} \\ &= \frac{1}{(2\pi i)^2} \int_{-i\infty}^{+i\infty} dz_1 dz_2 \frac{(m^2)^{\frac{d}{2} - a_1 - a_2 - a_3 - z_1 - z_2}}{(m^2 - p_1^2)^{-z_1} (-p_2^2)^{-z_2}} \\ & \quad \times \frac{\Gamma(-z_1) \Gamma(-z_2) \Gamma(a_2 + z_2) \Gamma(a_3 + z_1) \Gamma(a_1 + z_1 + z_2)}{\Gamma(a_1) \Gamma(a_2) \Gamma(a_3) \Gamma(d - a_1 - a_2 - a_3)} \\ & \quad \times \frac{\Gamma(d - a_1 - a_2 - 2a_3 - z_1) \Gamma(a_1 + a_2 + a_3 - \frac{d}{2} + z_1 + z_2)}{\Gamma(a_1 + a_2 + z_1 + 2z_2)}. \end{aligned} \quad (19)$$

Note that the exponents in Eqs. (18) and (19) need not be integer but may also depend on ϵ .

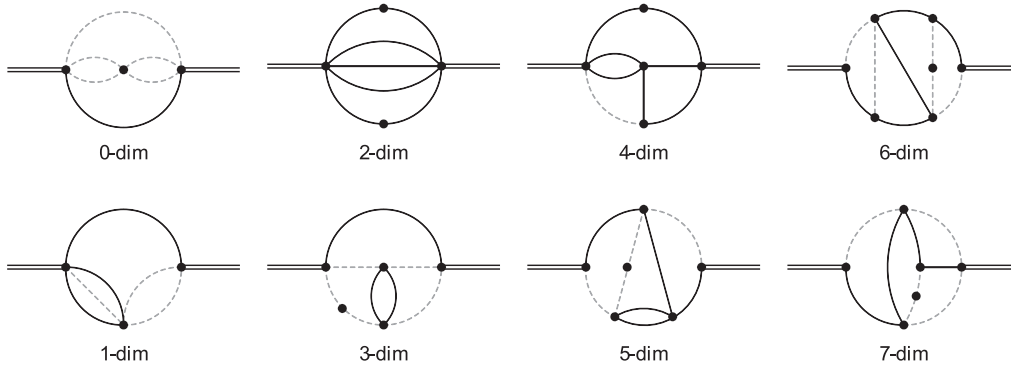


FIG. 5. Sample master integrals which are treated with the Mellin-Barnes method. The dimension of the Mellin-Barnes integration is specified below the diagrams.

(ii) *Decompose integral into products of building blocks.*

The derived building blocks are applied step by step until all momentum integrations are replaced by Mellin-Barnes integrals. For simple integrals one ends up with a two- or three-dimensional integration (cf. Fig. 5). In these cases a precision of about nine digits is achieved for the ϵ^6 terms. The coefficients of the lower ϵ -orders are more precise. We also encountered higher-dimensional integrals which lead to a lower precision. Some examples with five-, six- or even seven-dimensional integrations can be found in Fig. 5. For these cases one obtains about five digits for the ϵ^0 and two to three digits for the ϵ^3 term.

It is interesting to note that the decomposition into building blocks is not unique. In fact, different representations may have significantly different convergence properties which we exploited for some of the integrals.

Altogether we have treated 80 master integrals with the help of the described method. The results of the Mellin-Barnes integrals are usually quite precise for lower orders of the ϵ expansion and give several digits more than FIESTA provides. For 16 out of 80 integrals FIESTA produced more precise results for the higher orders in ϵ and we chose to compose “hybrid” results where the lower orders were taken from the Mellin Barnes (MB) integrals and the ϵ^3 or higher terms came from FIESTA.

For the preparation of the Mellin-Barnes integrals we use the package MB [68] together with its extensions discussed in Ref. [69]. For the numerical integration we use the integrator `cuhre` as implemented in the CUBA library [63]. As far as our experience goes the estimated uncertainty of `cuhre` is too small which can be seen by comparing the results of the numerical integration to (analytically) known results. Thus, we multiply the uncertainty by a factor 100 to be on the conservative side. For the higher-dimensional integrals we have also tried to use `vegas`; however, we could not increase the precision [70].

We have compared all 80 master integrals computed with the Mellin-Barnes method with the FIESTA results and

found good agreement for almost all ϵ coefficients within 3 standard deviations. However, in a few cases deviations up to seven sigma are observed which once again justifies the use of a conservative limit of ten sigma for the Monte Carlo uncertainty of FIESTA [70]. The systematic application of the Mellin-Barnes method is the main source for the improvements as compared to the results presented in Ref. [44].

The described procedure can, of course, only be applied to a subset of all master integrals. However, as mentioned above, in our basis these integrals provide the substantial part of the uncertainty to z_m in case we use the results based on FIESTA.

For the remaining 259 integrals (i.e. the ones which are neither known analytically nor treated with the Mellin-Barnes method) we use the FIESTA result. When inserting the master integrals we keep track of all uncertainties and combine them in quadrature in the final expression. We interpret the resulting uncertainty as a standard deviation and multiply it by 10 (as justified above) in the final result for the relation between the $\overline{\text{MS}}$ and on-shell quark mass. Note that, if we add the uncertainties from the individual contributions linearly we obtain an uncertainty which is about five times larger than the uncertainty resulting from the quadratic combination. For example, $z_m^{(4)}$ for $N_c = 3$ and $n_l = 5$ reads -871.732 ± 0.180 for quadratic and -871.732 ± 0.872 for the linear combination (without security factor 10).

III. RESULTS FOR THE $\overline{\text{MS}}$ -ON-SHELL RELATION

As an outcome of the procedure discussed in the previous section we obtain bare four-loop results for $\Sigma_V(q^2 = M_q^2) + \Sigma_S(q^2 = M_q^2)$ which still contain fourth-order poles in the regularization parameter ϵ . Furthermore, uncertainties from each ϵ order of the numerically evaluated master integrals are present in the expression. The individual uncertainties are eventually combined quadratically to obtain the overall uncertainty. It is obvious that the latter is sensitive to the following choices:

- (i) Set $N_c = 3$ (and optionally also a value for n_l) before combining the uncertainties from the master integrals.
- (ii) Parametrize $\Sigma_V + \Sigma_S$ in terms of generic N_c and n_l .
- (iii) Parametrize $\Sigma_V + \Sigma_S$ in terms of $\text{SU}(N_c)$ Casimir invariants.

In this section we discuss the three options. Note that we interpret the final uncertainty as a standard deviation which we multiply by a factor 10 to be on the conservative side.

It is convenient to present results for the finite relation between the $\overline{\text{MS}}$ and on-shell mass. It is obtained after

renormalization of the quark mass in the on-shell and the strong coupling constant in the $\overline{\text{MS}}$ scheme using three-loop renormalization constants. Whereas α_s is renormalized by a simple multiplicative factor it is convenient to generate the mass counterterm contribution at the same time as the lower-order contributions. A finite quantity is obtained after dividing the (parameter renormalized) Z_m^{OS} by $Z_m^{\overline{\text{MS}}}$, as discussed around Eq. (10).

To get a sense of the quality of the cancellations of the poles we present in the following table results for three typical contributions to $z_m^{(4)}$ ($\mu^2 = M^2$).

	$z_m^{(4)}$ for $N_c = 3, n_l = 5$	coef. of N_c^4 term	coef. of C_F^4 term
ϵ^{-4}	-0.00001 ± 0.00002	-0.0000002 ± 0.0000002	-0.000006 ± 0.000013
ϵ^{-3}	0.0003 ± 0.0002	0.000002 ± 0.000002	0.0001 ± 0.0001
ϵ^{-2}	-0.0002 ± 0.0018	0.000001 ± 0.000016	-0.0007 ± 0.0009
ϵ^{-1}	0.0044 ± 0.0191	0.00002 ± 0.00018	0.0005 ± 0.0081
ϵ^0	-871.732 ± 0.180	-51.181 ± 0.002	-6.983 ± 0.081

Note that the uncertainties are the ones returned from the numerical integration without introducing any security factor. Still, all pole coefficients are 0 within 1 standard deviation which shows that the factor 10 applied to the final results presented below is conservative.

From now on we only consider ϵ^0 terms and choose $\mu^2 = M^2$ (for z_m) or $\mu^2 = m^2(\mu^2)$ (for c_m). The renormalization scale dependent terms can be computed analytically using renormalization group techniques; they are given in Appendix C.

A. Results for $N_c = 3$

We start with specifying both N_c and n_l before combining the uncertainties of the master integrals. The results for $z_m^{(4)}(M)$ and $c_m^{(4)}(m)$ for $N_c = 3$ are shown in Table I. Note that for the physically interesting cases $n_l = 4, 5$ and 6 we find a relative uncertainty between 0.1% and 0.2%.

From Table I one observes that the uncertainty has only a very mild dependence on n_l . Thus, to a good approximation we can write $z_m^{(4)}$ in the form⁶

$$z_m^{(4)} = -3654.15 \pm 1.64 + (756.942 \pm 0.040)n_l - 43.4824n_l^2 + 0.678141n_l^3. \quad (20)$$

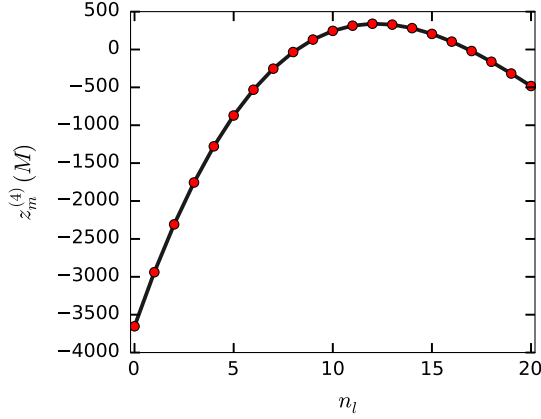
In Fig. 6 we plot Eq. (20) for n_l between 0 and 20 and combine the data points for integer n_l to guide the eye. It is interesting to note that the four-loop coefficient $z_m^{(4)}$ becomes positive between $n_l = 9$ and $n_l = 16$. Close to

these values of n_l (i.e. for $n_l = 8$ and $n_l = 17$) the absolute value of $z_m^{(4)}$ is quite small and thus the relative uncertainty exceeds 5%. The range for n_l where the four-loop coefficient changes sign coincides with the one for the so-called Banks-Zaks fixed point for the QCD beta function [71]. However, we are not aware of a deeper connection which might be a subject for further studies.

TABLE I. Results for $z_m^{(4)}(M)$ and $c_m^{(4)}(m)$ for $N_c = 3$ and $0 \leq n_l \leq 20$.

n_l	$z_m^{(4)}(M)$	$c_m^{(4)}(m)$
0	-3654.15 ± 1.64	3567.60 ± 1.64
1	-2940.01 ± 1.67	2864.60 ± 1.67
2	-2308.77 ± 1.70	2244.32 ± 1.70
3	-1756.36 ± 1.74	1702.70 ± 1.74
4	-1278.70 ± 1.77	1235.66 ± 1.77
5	-871.73 ± 1.80	839.14 ± 1.80
6	-531.39 ± 1.84	509.07 ± 1.84
7	-253.59 ± 1.87	241.37 ± 1.87
8	-34.28 ± 1.91	31.99 ± 1.91
9	130.62 ± 1.94	-123.15 ± 1.94
10	245.17 ± 1.98	-228.12 ± 1.98
11	313.45 ± 2.01	-286.98 ± 2.01
12	339.51 ± 2.05	-303.81 ± 2.05
13	327.44 ± 2.08	-282.68 ± 2.08
14	281.30 ± 2.12	-227.64 ± 2.12
15	205.16 ± 2.16	-142.78 ± 2.16
16	103.09 ± 2.19	-32.15 ± 2.19
17	-20.85 ± 2.23	100.16 ± 2.23
18	-162.58 ± 2.26	250.10 ± 2.26
19	-318.03 ± 2.30	413.59 ± 2.30
20	-483.15 ± 2.34	586.56 ± 2.34

⁶Note that this is not a fit to Table I.


 FIG. 6. n_l dependence of $z_m^{(4)}(M)$.

The four-loop coefficient of the inverted relation, $c_m^{(4)}$, which is basically obtained from negative $z_m^{(4)}$ plus some products of lower order contributions, shows a similar behavior except for the overall sign. It has, in particular, the same uncertainty, as can be seen in the last column of Table I. The explicit n_l dependence reads

$$c_m^{(4)} = 3567.60 \pm 1.64 - (745.721 \pm 0.040)n_l + 43.3963n_l^2 - 0.678141n_l^3. \quad (21)$$

For some applications it is useful to have control over all fermionic contributions, including the ones from closed fermion loops of mass M which we label by n_h . The corresponding result is shown in Table II where we present the coefficients of $n_l^i n_h^j$ for $i, j = 0, 1, 2, 3$ with $i + j \leq 3$.

B. Results for generic N_c

In a next step we do not specify numerical values for N_c and n_l which leads to 23 nonzero color structures. For the corresponding coefficients we obtain

 TABLE II. $z_m^{(4)}$ decomposed into coefficients of $n_l^i n_h^j$.

$n_l^0 n_h^0$	-3678.28 ± 1.63
$n_l^0 n_h^1$	23.63 ± 0.12
$n_l^0 n_h^2$	0.5273 ± 0.0027
$n_l^0 n_h^3$	-0.02484 ± 0.00000
$n_l^1 n_h^0$	757.64 ± 0.04
$n_l^1 n_h^1$	-0.6646 ± 0.0004
$n_l^1 n_h^2$	-0.03617 ± 0.00000
$n_l^2 n_h^0$	-43.47 ± 0.00
$n_l^2 n_h^1$	-0.01720 ± 0.00000
$n_l^3 n_h^0$	0.6781 ± 0.0000

$$\begin{aligned}
 z_m^{LLL/N_c^1} &= -0.25430, \\
 z_m^{LLN_c^1} &= 0.25430, \\
 z_m^{LL1/N_c^2} &= -0.14090, \\
 z_m^{LL1/N_c^1} &= 0.00645, \\
 z_m^{LNN_c^0} &= 5.58971, \\
 z_m^{LNN_c^1} &= -0.00645, \\
 z_m^{LNN_c^2} &= -5.44881, \\
 z_m^{L1/N_c^3} &= 0.1788 \pm 0.0333, \\
 z_m^{L1/N_c^2} &= -0.18076 \pm 0.00000, \\
 z_m^{L1/N_c^1} &= 0.9282 \pm 0.0445, \\
 z_m^{LN_c^0} &= 0.28392 \pm 0.00005, \\
 z_m^{LN_c^1} &= -32.7991 \pm 0.0109, \\
 z_m^{LN_c^2} &= -0.10316 \pm 0.00005, \\
 z_m^{LN_c^3} &= 31.69215 \pm 0.00124, \\
 z_m^{1/N_c^4} &= -0.4364 \pm 0.0503, \\
 z_m^{1/N_c^3} &= 0.821 \pm 0.121, \\
 z_m^{1/N_c^2} &= 0.1739 \pm 0.0738, \\
 z_m^{1/N_c^1} &= 0.645 \pm 0.161, \\
 z_m^{N_c^0} &= -0.614 \pm 0.175, \\
 z_m^{N_c^1} &= -2.6228 \pm 0.0415, \\
 z_m^{N_c^2} &= 52.0579 \pm 0.0808, \\
 z_m^{N_c^3} &= 1.15654 \pm 0.00424, \\
 z_m^{N_c^4} &= -51.1812 \pm 0.0161, \quad (22)
 \end{aligned}$$

where the notation used for the superscripts is self-explanatory.⁷ The n_l^3 and n_l^2 terms are known analytically and can be found in Ref. [67,72] (see Appendix E). Both for the linear- n_l and the n_l -independent contribution one obtains small (relative) uncertainties for the positive powers in N_c which dominate in the physical limit $N_c = 3$. This explains the small uncertainties of coefficients in the previous subsection.

From Eq. (22) one learns that for $N_c = 3$ the dominant uncertainty originates from $z_m^{N_c^2}$, followed by the N_c -independent term $z_m^{N_c^0}$.

As a cross-check we choose $N_c = 3$, fix n_l and use the coefficients of Eqs. (22) to compute $z_m^{(4)}$ combining all uncertainties again quadratically. We obtain the following results:

⁷Example: z_m^{L1/N_c^2} is the coefficient of n_l/N_c^2 ; “L” counts the factors n_l .

n_l	$z_m^{(4)}$
3	-1756.36 ± 1.52
4	-1278.70 ± 1.53
5	-871.73 ± 1.53

The central values are by construction identical to the corresponding entries in Table I; the uncertainties are even slightly smaller. This might happen since the uncertainties are added linearly when setting N_c and n_l to numerical values before combining the uncertainties from the individual c terms (cf. Sec. III A). As compared to adding the uncertainties in quadrature this might lead to larger (as in the case at hand) or smaller (see the next subsection) uncertainties.

C. Results in terms of Casimir color factors

This subsection is devoted to the most general results, namely z_m in the form of Eq. (15). For the coefficients of the 23 color structures we obtain

$$\begin{aligned}
 z_m^{FFFF} &= -6.983 \pm 0.805, \\
 z_m^{FFFA} &= 13.40 \pm 2.07, \\
 z_m^{FFAA} &= -11.17 \pm 1.74, \\
 z_m^{FAAA} &= -99.272 \pm 0.493, \\
 z_m^{d_{FA}} &= 0.39 \pm 1.07, \\
 z_m^{d_{FFL}} &= -0.937 \pm 0.178, \\
 z_m^{d_{FFH}} &= -3.924 \pm 0.642, \\
 z_m^{FFFL} &= -0.05094 \pm 0.00298, \\
 z_m^{FFAL} &= 9.26642 \pm 0.00454, \\
 z_m^{FAAL} &= 122.1872 \pm 0.0100, \\
 z_m^{FFLL} &= -2.25441, \\
 z_m^{FALL} &= -42.46326, \\
 z_m^{FLLL} &= 4.06885, \\
 z_m^{FFFH} &= -1.3625 \pm 0.0132, \\
 z_m^{FFAH} &= 14.9800 \pm 0.0334, \\
 z_m^{FAAH} &= -2.3597 \pm 0.0342, \\
 z_m^{FFHH} &= 1.65752 \pm 0.00031, \\
 z_m^{FAHH} &= -0.20934 \pm 0.00273, \\
 z_m^{FHHH} &= -0.14902 \pm 0.00000, \\
 z_m^{FFLH} &= -2.89209 \pm 0.00010, \\
 z_m^{FALH} &= 0.62076 \pm 0.00042, \\
 z_m^{FLLH} &= -0.10321, \\
 z_m^{FLHH} &= -0.21703 \pm 0.00000. \tag{23}
 \end{aligned}$$

The n_l^3 and n_l^2 terms are known analytically and can be found in Appendix E. The linear- n_l term is dominated by

z_m^{FAAL} which has an uncertainty below 0.01%. On the other hand, for z_m^{FFFL} the precision is only about 4%; however, the numerical impact is small, even for $N_c = 2$.

The contributions involving closed heavy quark loops are generally small and known to a precision of about 10% or better, the numerically dominant z_m^{FFAH} contribution even to about 1.3%.

There are five nonfermionic contributions, z_m^{FFFF} , z_m^{FFFA} , z_m^{FFAA} , z_m^{FAAA} and $z_m^{d_{FA}}$. The most precise one, z_m^{FAAA} , has by far the largest coefficient and furthermore the largest color factor. The three coefficients z_m^{FFFF} , z_m^{FFFA} and z_m^{FFAA} have an uncertainty between 11% and 15%. $z_m^{d_{FA}}$ is the worst known coefficient. Actually, within our precision we cannot claim whether it is positive or negative. Note, however, that not only the coefficient itself but also the color factor is numerically small as compared to others. For example, for $N_c = 3$ we have $d_F^{abcd} d_A^{abcd} / N_c = 15/6 = 2.5$ whereas $C_F C_A^3 = 36$. The current uncertainty of $z_m^{d_{FA}}$ is dominated by master integrals where we rely on the FIESTA results.

As a cross-check we insert the results from Eq. (23) into Eq. (15) and specify the color factors to their numerical values with $N_c = 3$. We add all uncertainties in quadrature and obtain

n_l	$z_m^{(4)}$
3	-1756.36 ± 36.3
4	-1278.70 ± 36.3
5	-871.73 ± 36.3

which has to be compared with the corresponding entries in Table I where $N_c = 3$ is chosen before combining the uncertainties from the individual master integrals. As expected, one observes the same central value; however, the uncertainties are significantly larger.

IV. APPLICATIONS

A. $\overline{\text{MS}}$ -on-shell transformation formulas

In the following we discuss the relation between the $\overline{\text{MS}}$ and on-shell quark mass and specify the number of massless quarks to the top, bottom and charm case.

Let us start with the version where the on-shell mass is computed from the $\overline{\text{MS}}$ mass. We use as input the following $\overline{\text{MS}}$ masses,

$$\begin{aligned}
 m_t(m_t) &= 163.508 \text{ GeV}, \\
 m_b(m_b) &= 4.163 \text{ GeV}, \\
 m_c(3 \text{ GeV}) &= 0.986 \text{ GeV}, \tag{24}
 \end{aligned}$$

where $m_t(m_t)$ is computed from $M_t = 173.34 \text{ GeV}$ [10] using four-loop accuracy. The $\overline{\text{MS}}$ masses for charm and bottom are taken from Ref. [3].

The values for the strong coupling are given by $\alpha_s^{(6)}(m_t) = 0.1085$, $\alpha_s^{(5)}(m_b) = 0.2253$, and $\alpha_s^{(4)}(3 \text{ GeV}) = 0.2540$. They have been computed from $\alpha_s^{(5)}(M_Z) = 0.1181$ using RunDec [46,47]. In the case of the charm quark we also provide results for $\mu = m_c(m_c)$ using the input values $m_c(m_c) = 1.279 \text{ GeV}$ and $\alpha_s^{(4)}(m_c) = 0.3872$. Note that the choice $\mu = 3 \text{ GeV}$ is preferable since it has the advantage that low renormalization scales $\mu \approx m_c$ are avoided.

In the following equations we list the results for the relations which convert the $\overline{\text{MS}}$ to the on-shell mass. For simplicity we set here and in the remainder of this section the uncertainty of the four-loop coefficient to 0.2% although it is for charm and bottom slightly smaller (see Table I). We obtain

$$\begin{aligned} M_t &= m_t(m_t)(1 + 0.4244\alpha_s + 0.8345\alpha_s^2 \\ &\quad + 2.375\alpha_s^3 + (8.615 \pm 0.017)\alpha_s^4) \\ &= 163.508 + 7.529 + 1.606 + 0.496 \\ &\quad + (0.195 \pm 0.0004) \text{ GeV}, \end{aligned} \quad (25)$$

$$\begin{aligned} M_b &= m_b(m_b)(1 + 0.4244\alpha_s + 0.9401\alpha_s^2 \\ &\quad + 3.045\alpha_s^3 + (12.685 \pm 0.025)\alpha_s^4) \\ &= 4.163 + 0.398 + 0.199 + 0.145 \\ &\quad + (0.136 \pm 0.0003) \text{ GeV}, \end{aligned} \quad (26)$$

$$\begin{aligned} M_c &= m_c(3 \text{ GeV})(1 + 1.133\alpha_s + 3.119\alpha_s^2 \\ &\quad + 10.981\alpha_s^3 + (51.419 \pm 0.102)\alpha_s^4) \\ &= 0.986 + 0.284 + 0.198 + 0.177 \\ &\quad + (0.211 \pm 0.0004) \text{ GeV}, \end{aligned} \quad (27)$$

$$\begin{aligned} M_c &= m_c(m_c)(1 + 0.4244\alpha_s + 1.0456\alpha_s^2 \\ &\quad + 3.757\alpha_s^3 + (17.480 \pm 0.035)\alpha_s^4) \\ &= 1.279 + 0.210 + 0.200 + 0.279 \\ &\quad + (0.503 \pm 0.001) \text{ GeV}, \end{aligned} \quad (28)$$

where the renormalization scale of α_s in each equation is identical to the one specified for the $\overline{\text{MS}}$ quark mass in the prefactor of the first lines in each equation.

One observes a good convergence for the top quark where the coefficients steadily decrease; the four-loop coefficient is more than a factor 2 smaller than the three-loop one. This is different for charm and bottom where the two-, three- and four-loop coefficients are of the same order of magnitude. In Eq. (28) (where $\mu^2 = m_c^2$ has been chosen) the four-loop coefficient is even almost twice as large as the three-loop coefficient.

For convenience we also present the inverted relation of Eq. (25) which is given by

$$\begin{aligned} m_t(m_t) &= M_t(1 - 0.4244\alpha_s - 0.9246\alpha_s^2 - 2.593\alpha_s^3 \\ &\quad - (8.949 \pm 0.018)\alpha_s^4) \\ &= 173.34 - 7.924 - 1.859 - 0.562 \\ &\quad - (0.209 \pm 0.0004) \text{ GeV}, \end{aligned} \quad (29)$$

where $\alpha_s \equiv \alpha_s(M_t) = 0.1077$. We refrain from providing the analogue equations for charm and bottom since this would require specifying the pole masses.

B. Relation between $\overline{\text{MS}}$ and threshold mass

The threshold masses are constructed such that the relation to the $\overline{\text{MS}}$ mass is well behaved in perturbation theory. It is illustrating to examine the cancellations which take place between the coefficients in the $\overline{\text{MS}}$ -OS relation and the ones in the relation of the OS and threshold mass. For example, in the case for the bottom quark mass we have for the PS mass

$$\begin{aligned} m_b^{\text{PS}}(\mu_f = 2 \text{ GeV}) &= 4.163 + (0.399 - 0.191) \\ &\quad + (0.199 - 0.120) + (0.145 - 0.114) \\ &\quad + (0.1364 - 0.1368 \pm 0.0003) \text{ GeV} \\ &= 4.163 + 0.207 + 0.080 + 0.032 \\ &\quad - (0.0004 \pm 0.0003) \text{ GeV}, \end{aligned} \quad (30)$$

where the second terms inside the round brackets after the first equality sign originate from the PS-OS relation. As expected due to the very definition of the PS mass, one observes a significant cancellation between the coefficients of the PS-OS and PS- $\overline{\text{MS}}$ relation. The cancellation becomes stronger at higher loop order. In particular, at four loops one observes a cancellation of three significant digits, which is the reason why four digits after the comma are provided. Note that the details of the cancellations depend on μ_f , as we discuss in Sec. IV C.

After the second equality sign the numbers in the round brackets are added. One observes a nice convergence behavior with decreasing coefficients which has to be compared to the OS- $\overline{\text{MS}}$ relation where the three- and four-loop coefficients have the same order of magnitude, cf. Eq. (26). The four-loop coefficient in Eq. (30) only amounts to -0.4 MeV which is actually of the same order of magnitude as the uncertainty. Note, however, that both the central value and the uncertainty are far below the expected precision of the $\overline{\text{MS}}$ bottom quark mass within the foreseeable future.

The analogue equation to (30) for the top quark reads

$$\begin{aligned} m_t^{\text{PS}}(\mu_f = 80 \text{ GeV}) &= 163.508 + (7.531 - 3.685) + (1.607 - 0.989) \\ &\quad + (0.495 - 0.403) + (0.195 - 0.211 \pm 0.0004) \text{ GeV} \\ &= 163.508 + 3.847 + 0.618 + 0.092 - (0.016 \pm 0.0004) \text{ GeV}. \end{aligned} \quad (31)$$

Also here one observes a drastic reduction of the correction terms when going to higher orders. In fact, the last term amounts to only 16 MeV instead of 200 MeV in Eq. (25).

For the 1S mass we obtain the following perturbative relations to the $\overline{\text{MS}}$ bottom and top mass,

$$\begin{aligned} m_b^{1\text{S}} &= 4.163 + (0.399 - 0.047) + (0.195 - 0.072) + (0.139 - 0.100) + (0.129 - 0.137 \pm 0.0003) \text{ GeV} \\ &= 4.163 + 0.352 + 0.123 + 0.039 - (0.008 \pm 0.0003) \text{ GeV}, \\ m_t^{1\text{S}} &= 163.508 + (7.531 - 0.428) + (1.588 - 0.368) + (0.479 - 0.262) + (0.185 - 0.174 \pm 0.0004) \text{ GeV} \\ &= 163.508 + 7.103 + 1.220 + 0.217 + (0.011 \pm 0.0004) \text{ GeV}, \end{aligned} \quad (32)$$

where the first and second number in the bracket originates from the OS- $\overline{\text{MS}}$ and OS-1S relation, respectively. Furthermore, we order the terms according to the ϵ expansion as defined in Refs. [5–7]. It is interesting to note that at leading order (LO) (first round bracket) the contribution from the OS-1S relation amounts only to a few per cent of the OS- $\overline{\text{MS}}$ relation. At N³LO, however, it is more than 90% both for bottom and top.

Similar results to those presented in Eqs. (30), (31) and (32) for bottom and top are also obtained for the charm quark in case $\mu = 3 \text{ GeV}$ is chosen for the renormalization scale. On the other hand, in the case when the relation of the threshold mass to $m_c(m_c)$ is computed the four-loop term exceeds the three-loop one. We furthermore observe that the relations to the RS and RS' masses behave very similar to the PS and 1S masses. We refrain from providing explicit results which are easily obtained with the help of RunDec [46] and CRunDec [47].

In practice a threshold quark mass is extracted from comparison of experimental measurements and theory predictions. Afterwards it is converted to the $\overline{\text{MS}}$ quark mass. In Table III we show the results for the scale invariant $\overline{\text{MS}}$ quark masses $m_q(m_q)$ ($q = t, b, c$) and $m_c(3 \text{ GeV})$ using one- to four-loop accuracy for the conversion. The input values for the threshold masses (which are provided at the top of each table) are chosen such that the four-loop results agree with the input values discussed in Eq. (24). For the top quark a rapid convergence is observed with four-loop contributions between 10 and 20 MeV. The situation is similar for the bottom quark where the four-loop term amounts to at most 8 MeV for the case of the 1S mass. As already mentioned above, the four-loop term for the case where $m_c(m_c)$ is computed from the threshold masses is larger than the three-loop contribution which is different for $m_c(3 \text{ GeV})$ where the four-loop term is

smaller by up to a factor 4. Thus, even in this case we observe a reasonable convergence of the perturbative series; for the PS and RS masses the N³LO corrections are even below 10 MeV.

The results in Table III show that perturbatively well-behaved quark mass relations are obtained after introducing threshold masses. To exploit them at third order in perturbation theory, which is mandatory due to current precision reached for the quark masses, it is necessary to use the four-loop relation between the on-shell and $\overline{\text{MS}}$ quark mass for the construction of the $\overline{\text{MS}}$ -threshold mass relation.

To obtain the results in Table III we have set the renormalization scale in the relation between the threshold and $\overline{\text{MS}}$ mass to the quark mass itself or to 3 GeV. As an alternative one could also apply the conversion relation at some intermediate scale μ and then run with four-loop accuracy in the $\overline{\text{MS}}$ scheme for either the scale invariant mass or to $\mu = 3 \text{ GeV}$ for the charm quark. The corresponding results are shown in Fig. 7 where $m_t(m_t)$, $m_b(m_b)$ and $m_c(3 \text{ GeV})$ are shown as a function of the intermediate scale μ . The panels on the left show the results for the PS mass for the one- to four-loop analysis. In all three cases one observes a rapid convergence when including higher order corrections resulting in an almost horizontal, i.e. μ -independent, result at four loops.

The panels on the right compare the various threshold masses at three and four loops. Note that by construction the four-loop curves coincide for $\mu = m_q(m_q)$ for top and bottom and for $\mu = 3 \text{ GeV}$ for charm. In all cases one observes that the four-loop curves are significantly flatter than the three-loop results. Particularly good results are obtained for the top quark in panel (b) where in a large range the four-loop results lie on top of each other. The four-loop curves in the case of the bottom quark show

TABLE III. $m_q(m_q)$ ($q = t, b, c$) in GeV [see (a)–(c)] and $m_c(3 \text{ GeV})$ (d) computed from the PS, 1S, RS and RS' quark mass using LO to N³LO accuracy. The numbers in the last line are obtained by taking into account the uncertainty of the four-loop coefficient, i.e., it is increased by 0.2%. This leads to a shift of at most 1 MeV. The factorization scales for the PS, RS and RS' masses are set to 2 GeV for bottom and charm. For the top quark we use $\mu_f = 80 \text{ GeV}$ for the PS, RS and RS' masses.

(a) $m_t(m_t)$				
Input	$m^{\text{PS}} =$	$m^{1\text{S}} =$	$m^{\text{RS}} =$	$m^{\text{RS}'} =$
No. of loops	168.049	172.060	166.290	171.785
1	164.174	164.904	163.702	164.226
2	163.580	163.727	163.520	163.591
3	163.492	163.519	163.490	163.500
4	163.508	163.508	163.508	163.508
4 ($\times 1.002$)	163.507	163.507	163.507	163.507
(b) $m_b(m_b)$				
Input	$m^{\text{PS}} =$	$m^{1\text{S}} =$	$m^{\text{RS}} =$	$m^{\text{RS}'} =$
No. of loops	4.481	4.668	4.364	4.692
1	4.266	4.308	4.210	4.286
2	4.191	4.192	4.173	4.196
3	4.163	4.155	4.159	4.165
4	4.163	4.163	4.163	4.163
4 ($\times 1.002$)	4.163	4.163	4.163	4.163
(c) $m_c(m_c)$				
Input	$m^{\text{PS}} =$	$m^{1\text{S}} =$	$m^{\text{RS}} =$	$m^{\text{RS}'} =$
No. of loops	1.130	1.513	1.035	1.351
1	1.255	1.342	1.249	1.146
2	1.230	1.250	1.273	1.276
3	1.235	1.214	1.249	1.250
4	1.279	1.279	1.279	1.279
4 ($\times 1.002$)	1.278	1.278	1.278	1.278
(d) $m_c(3 \text{ GeV})$				
Input	$m^{\text{PS}} =$	$m^{1\text{S}} =$	$m^{\text{RS}} =$	$m^{\text{RS}'} =$
No. of loops	1.153	1.545	1.043	1.357
1	1.077	1.261	1.028	1.074
2	1.021	1.117	1.008	1.020
3	0.993	1.032	0.992	0.995
4	0.986	0.986	0.986	0.986
4 ($\times 1.002$)	0.986	0.986	0.986	0.986

stronger variations below, say, $\mu = 2.5 \text{ GeV}$. Here the PS, RS and RS' results are quite close together whereas the 1S curve shows a quite strong rise for $\mu \rightarrow 2 \text{ GeV}$. Note that the scale on the y axis for the charm plot covers a bigger range than for the bottom quark. Nevertheless the four-loop curve shows a quite flat behavior. One observes again that the 1S curve deviates from the remaining ones.

C. μ_f dependence of PS, RS and RS' mass

In this section we study the dependence of the PS, RS and RS' mass on the factorization scale μ_f . To do this we

use $m_t(m_t)$, $m_b(m_b)$, $m_c(m_c)$ and $m_c(3 \text{ GeV})$ from Eq. (24) and compute the threshold masses for the given value of μ_f to four-loop accuracy. This value is then used as starting point for the computation of the $\overline{\text{MS}}$ mass at one- to four-loop order as a function of μ_f . In Fig. 8 the three- (black) and four-loop (red) contributions to the conversion formula are plotted for the PS (solid), RS (short dashes) and RS' (long dashes) masses. In the case of the top quark the default scale for the PS mass suggested in Ref. [4] is $\mu_f = 20 \text{ GeV}$. For this value the four-loop contribution amounts to about -50 MeV . One observes that the perturbative conversion formula is better behaved for larger values of μ_f . In fact, the four-loop term vanishes for $\mu_f \approx 50 \text{ MeV}$ and amounts to about $+10 \text{ MeV}$ for $\mu_f \approx 80 \text{ MeV}$, a value suggested in Ref. [14] in the context of top quark pair production close to threshold. Similar conclusions also hold for the RS and RS' masses.

For the bottom quark the general behavior of the three- and four-loop correction terms is similar to the top quark case. Here, the suggested default value of $\mu_f = 2 \text{ GeV}$ [4,8] seems to be a good choice from the perturbative point of view.

For completeness we show in Fig. 8 the corresponding results for the charm quark masses $m_c(m_c)$ and $m_c(3 \text{ GeV})$. Here, the results are less conclusive, in particular, for $m_c(m_c)$. Over a large range of μ_f the four-loop term is even larger than the three-loop contribution which is a sign that the formalism should not be applied to $m_c(m_c)$. The situation is better when $m_c(3 \text{ GeV})$ is considered, which is probably due to the smaller values of α_s [which increases significantly when going from $\mu = 3 \text{ GeV}$ to $\mu = m_c(m_c) \approx 1.3 \text{ GeV}$]. For $m_c(3 \text{ GeV})$ the four-loop contribution is always smaller than the three-loop term; however, it comes close to 0 only for values near $\mu_f \approx 3 \text{ GeV}$.

D. c_m in terms of $\alpha_s^{(n_i)}$

For certain applications (see, e.g. Ref. [2]) it is necessary to express the $\overline{\text{MS}}$ -on-shell relation in terms of $\alpha_s^{(n_i)}$ instead of $\alpha_s^{(n_i+1)}$. It is obtained by using the decoupling relation for α_s , which is given by⁸

$$\alpha_s^{(n_i+1)} = \zeta_{\alpha_s} \alpha_s^{(n_i)}, \quad (33)$$

with

$$\zeta_{\alpha_s} = 1 + \frac{1}{6} \frac{\alpha_s^{(n_i)}}{\pi} \log\left(\frac{\mu^2}{m^2(\mu^2)}\right) + \mathcal{O}(\alpha_s^2), \quad (34)$$

⁸The formulas of this subsection and the ones of the appendixes (except Appendix E) can be found on the website https://www.ttp.kit.edu/_media/progdata/2016/ttp16-023.tgz and also see Supplemental Material [73].

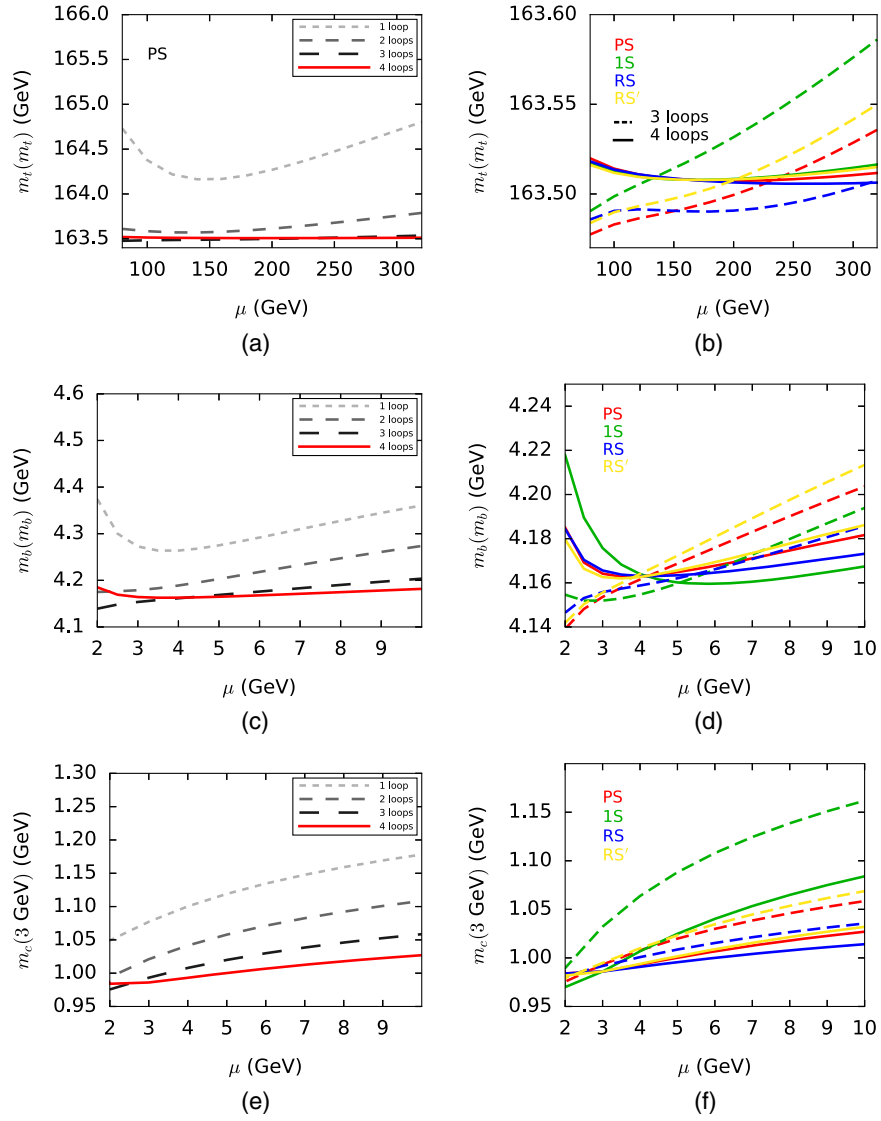


FIG. 7. (a) $\overline{\text{MS}}$ top quark mass $m_t(m_t)$ computed from the PS mass with LO, next-to-leading order, NNLO and N^3LO accuracy as a function of the renormalization scale used in the $\overline{\text{MS}}$ -threshold mass relation. (b) $\overline{\text{MS}}$ top quark mass $m_t(m_t)$ computed from the PS, 1S, RS and RS' mass with NNLO (dashed) and N^3LO (solid line) accuracy as a function of the renormalization scale used in the $\overline{\text{MS}}$ -threshold mass relation. At the right end of the plot the lines from bottom to top correspond to the RS, PS, RS' 1S mass. (c)–(f) show the results for bottom and charm. For the bottom quark the four-loop result for the 1S mass is below (above) the others for high (low) values of μ .

where results up to four-loop order can be found in Refs. [74,75]. In our case we only need three-loop corrections which have been computed for the first time in Ref. [76]. Inserting Eq. (33) into the equation for z_m leads to

$$c_m(n_l) = c_m(n_l + 1)|_{\alpha_s^{(n_l+1)} \rightarrow \alpha_s^{(n_l)}} + \delta c_m(n_l), \quad (35)$$

with

$$\delta c_m^{(2)} = \frac{l_\mu^2}{6} + \frac{2l_\mu}{9}, \quad (36)$$

$$\delta c_m^{(3)} = \left[\left(-\frac{\zeta_3}{18} + \frac{\pi^2}{9} + \frac{117}{32} + \frac{1}{27} \pi^2 \log(2) \right) l_\mu + \frac{5l_\mu^3}{8} + \frac{25l_\mu^2}{9} + \left\{ -\frac{l_\mu^3}{36} - \frac{13l_\mu^2}{108} + \left(-\frac{71}{432} - \frac{\pi^2}{54} \right) l_\mu \right\} n_l - \frac{11}{54} \right], \quad (37)$$

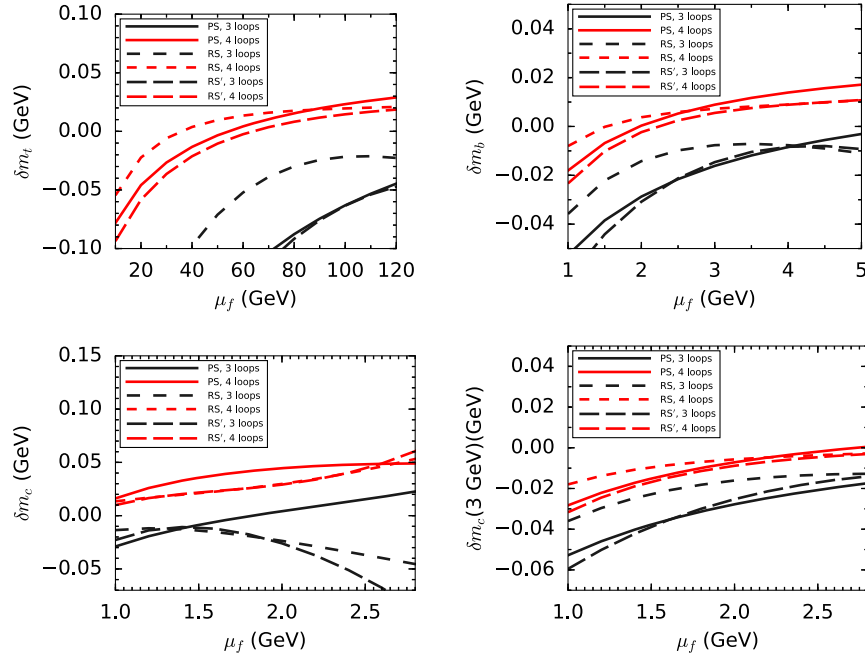


FIG. 8. Three- (black, lower three curves in each plot) and four-loop (red, upper three curves in each plot) contribution in transition from PS, RS and RS' mass to $m_q(m_q)$ and $m_c(3 \text{ GeV})$ as a function of the factorization scale μ_f .

$$\begin{aligned}
 \delta c_m^{(4)} = & \left[l_\mu \left(-\frac{110a_4}{27} - \frac{1439\pi^2\zeta_3}{864} + \frac{107515\zeta_3}{27648} + \frac{1975\zeta_5}{432} - \frac{695\pi^4}{15552} + \frac{676601\pi^2}{77760} \right. \right. \\
 & + \left. \frac{18532949}{373248} - \frac{55\log^4(2)}{324} - \frac{11}{81}\pi^2\log^2(2) - \frac{271}{162}\pi^2\log(2) \right) \\
 & + n_l \left\{ l_\mu \left(\frac{4a_4}{27} - \frac{241\zeta_3}{144} + \frac{61\pi^4}{3888} - \frac{1057\pi^2}{1296} - \frac{502145}{93312} + \frac{\log^4(2)}{162} \right. \right. \\
 & + \left. \frac{1}{81}\pi^2\log^2(2) - \frac{11}{162}\pi^2\log(2) \right) + \left(-\frac{7\zeta_3}{18} - \frac{25\pi^2}{108} - \frac{11233}{2592} - \frac{1}{54}\pi^2\log(2) \right) l_\mu^2 \\
 & - \frac{83l_\mu^4}{432} - \frac{1171l_\mu^3}{864} + \frac{11\pi^2}{648} + \frac{12295}{46656} \left. \right\} + \frac{83099\zeta_3}{20736} + \left(-\frac{17\zeta_3}{18} + \frac{19\pi^2}{18} + \frac{442177}{10368} \right. \\
 & + \left. \frac{19}{54}\pi^2\log(2) \right) l_\mu^2 + \frac{431l_\mu^4}{216} + \frac{8869l_\mu^3}{648} + n_l^2 \left\{ \left(\frac{7\zeta_3}{108} + \frac{13\pi^2}{648} + \frac{2353}{46656} \right) l_\mu + \frac{l_\mu^4}{216} \right. \\
 & + \left. \frac{13l_\mu^3}{432} + \left(\frac{89}{1296} + \frac{\pi^2}{108} \right) l_\mu^2 \right\} - \frac{11\pi^2}{108} - \frac{209567}{23328} - \frac{11}{324}\pi^2\log(2) \left. \right], \quad (38)
 \end{aligned}$$

with

$$l_\mu = \log\left(\frac{\mu^2}{m^2(\mu)}\right), \quad a_n = \text{Li}_n\left(\frac{1}{2}\right). \quad (39)$$

V. CONCLUSIONS

The main result of this paper is the calculation of the four-loop coefficient in the relation between the $\overline{\text{MS}}$ and on-shell heavy quark mass. Up to the reduction to master integrals the calculation is performed analytically.

However, most of the master integrals are only known numerically. For QCD, we managed to obtain an uncertainty of 0.2% for the four-loop coefficient.

We have also computed the coefficients of the individual color structures. It is interesting to note that the large coefficients (z_m^{FAAA} and z_m^{FAAL}) are known to high precision and furthermore also have large color factors. Thus, they dominate the numerical result obtained after specifying N_c , in particular, the physical result for $N_c = 3$. Some coefficients are known to high relative precision; others have uncertainties of about

30%. There is one coefficient ($z_m^{d_{FA}}$) with an uncertainty which is larger than the central value. Fortunately, it has only a minor numerical contribution to z_m .

In this paper several applications have been discussed. Among them is the numerical analysis of the heavy quark relation for the top, bottom and charm quark. Furthermore, the relations between the $\overline{\text{MS}}$ and several threshold masses are investigated. We have shown that the latter have well-behaved perturbative expansions, in particular, for the top and bottom quark. We have furthermore investigated the dependence of the PS, RS and RS' masses on the factorization scale. It turns out that for bottom and charm $\mu_f = 2$ GeV is a reasonable choice. For the top quark we observe that for $\mu_f = 80$ GeV the four-loop corrections are small. The numerical results presented in Sec. IV are easily reproduced with the help of RunDec [46] and CRunDec [47] where the latest results for the mass relations are implemented.

ACKNOWLEDGMENTS

We are thankful to Tobias Huber for advice on numerical evaluation of MB integrals and to Kirill Melnikov for carefully reading the manuscript. We thank the HLRS and the Supercomputing Center of Lomonosov Moscow State University [77] for providing computing time used for the numerical computations with FIESTA. P.M. was supported in part by the EU network Grant No. HIGGSTOOLS PITN-GA-2012-316704. The work of V.S. was supported by the Alexander von Humboldt Foundation (Humboldt Forschungspreis).

APPENDIX A: INTEGRAL FAMILIES

Graphical representation of the 102 integral families is shown in Figs. 9–11. They are obtained from Fig. 2 by introducing a throughgoing massive line. Note that tables are only required for 100 families since the color factors of the diagrams mapped to two families are 0.

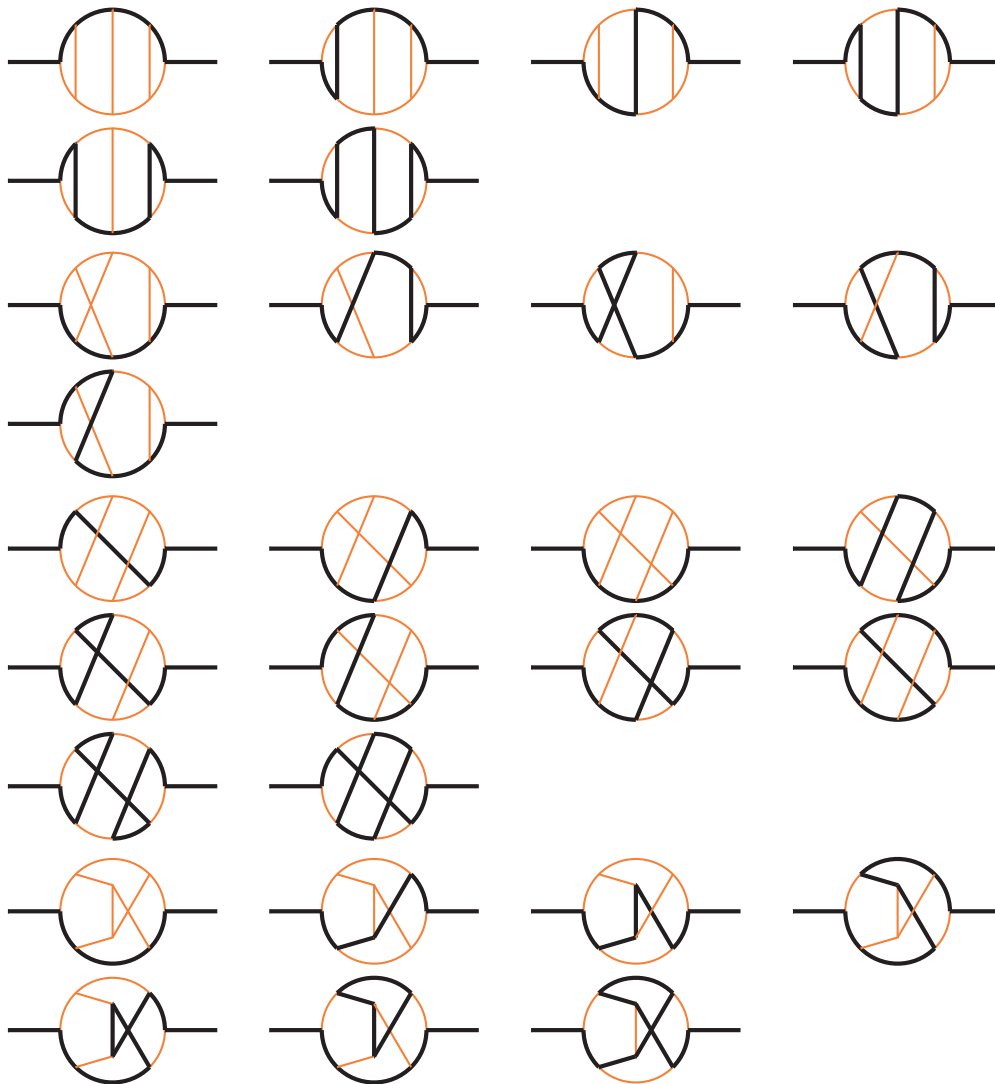


FIG. 9. Integral families needed at four-loop order. Thick black lines indicate massive particles and thin orange lines massless particles.

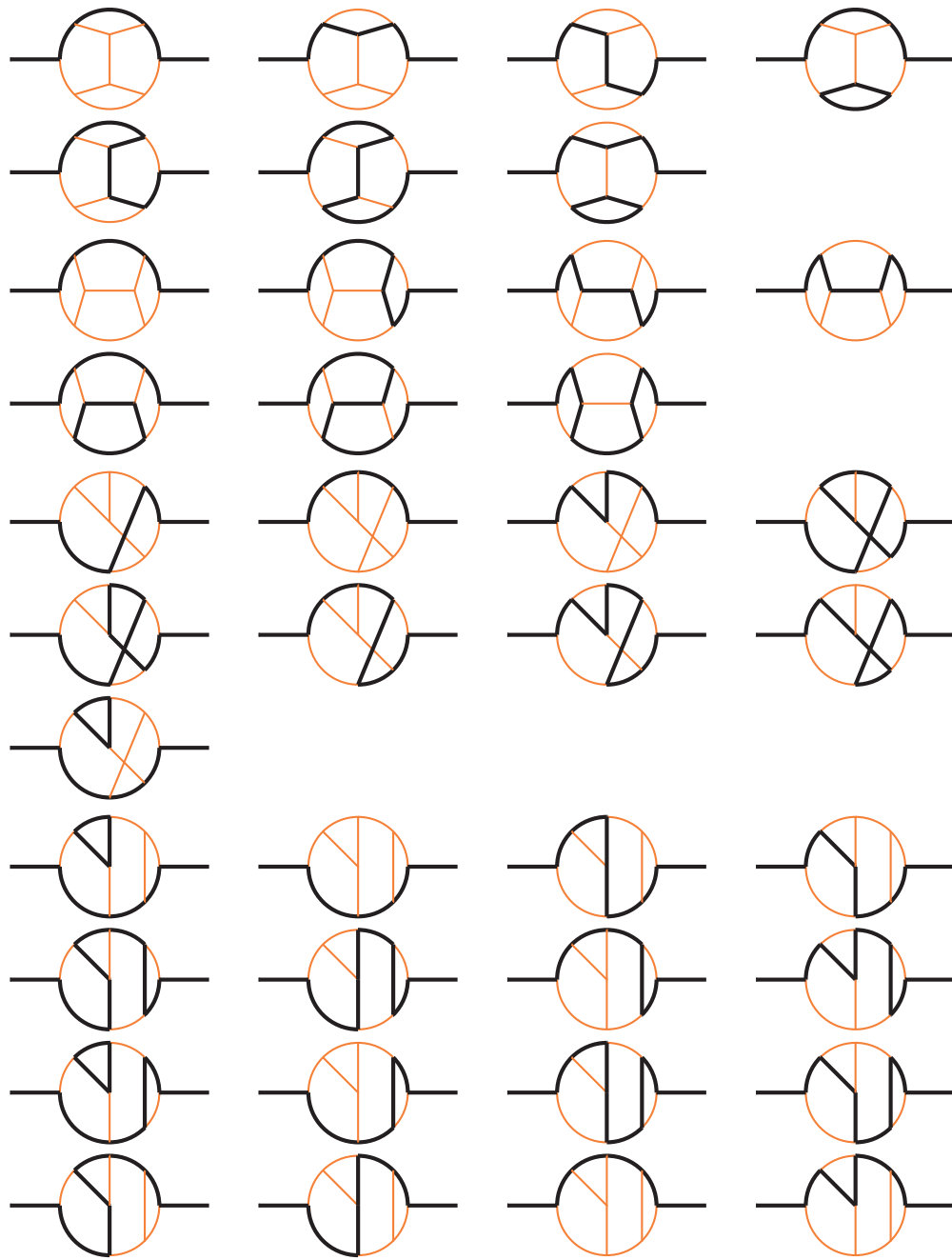


FIG. 10. Four-loop families (continued).

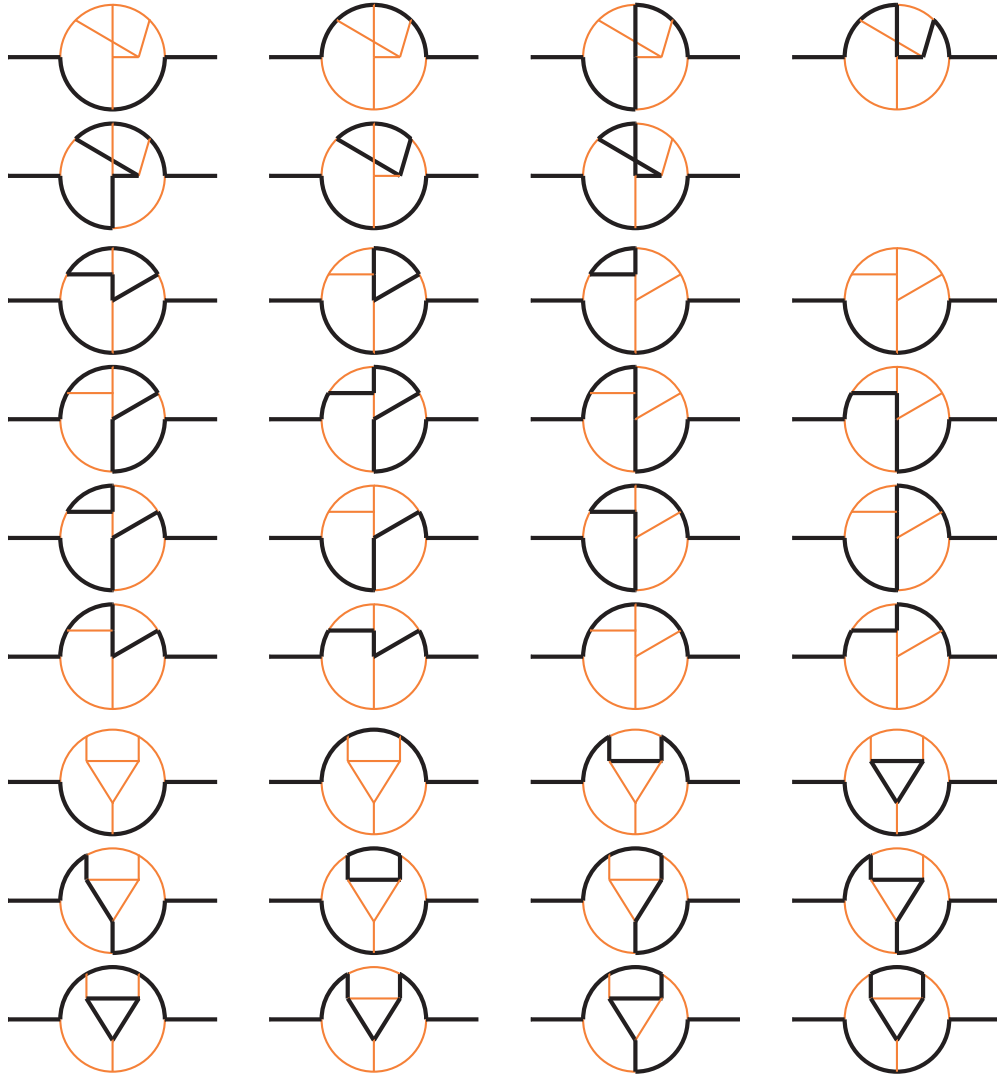


FIG. 11. Four-loop families (continued).

APPENDIX B: ANALYTIC RESULTS FOR z_m UP TO THREE LOOPS

In this appendix we present analytic results for z_m up to three loops including higher order terms in ϵ which might be important in case the relation between the $\overline{\text{MS}}$ and on-shell mass is used in divergent expressions. For $\mu^2 = M^2$ our results read

$$\begin{aligned}
 z_m^{(1)} &= \left(\frac{\zeta(3)}{3} - 8 - \frac{\pi^2}{6} - \frac{3\pi^4}{640} \right) \epsilon^3 C_F + \left(\frac{\zeta(3)}{4} - 4 - \frac{\pi^2}{12} \right) \epsilon^2 C_F + \left(-2 - \frac{\pi^2}{16} \right) \epsilon C_F - C_F, \\
 z_m^{(2)} &= \epsilon \left(C_A C_F \left(6a_4 + \frac{13\zeta_3}{4} - \frac{7\pi^4}{80} + \frac{271\pi^2}{1152} - \frac{8581}{768} + \frac{\log^4(2)}{4} + \frac{1}{2} \pi^2 \log^2(2) - \frac{3}{2} \pi^2 \log(2) \right) \right. \\
 &\quad + C_F^2 \left(-12a_4 - \frac{33\zeta_3}{4} + \frac{7\pi^4}{40} - \frac{213\pi^2}{128} - \frac{91}{256} - \frac{\log^4(2)}{2} - \pi^2 \log^2(2) + 3\pi^2 \log(2) \right) \\
 &\quad \left. + TC_F \left(-\frac{7\zeta_3}{2} - \frac{227\pi^2}{288} + \frac{1133}{192} + \pi^2 \log(2) \right) n_h + \left(\zeta_3 + \frac{97\pi^2}{288} + \frac{581}{192} \right) TC_F n_l \right)
 \end{aligned}$$

$$\begin{aligned}
 & + \epsilon^2 \left(C_A C_F \left(36a_4 + 36a_5 - \frac{11\pi^2 \zeta_3}{16} + \frac{3929\zeta_3}{288} - \frac{609\zeta_5}{16} - \frac{1087\pi^4}{2560} + \frac{1537\pi^2}{2304} - \frac{58543}{1536} - \frac{3\log^5(2)}{10} + \frac{3\log^4(2)}{2} \right. \right. \\
 & - \left. \pi^2 \log^3(2) + 3\pi^2 \log^2(2) + \frac{13}{60} \pi^4 \log(2) - \frac{11}{2} \pi^2 \log(2) \right) + C_F^2 \left(-72a_4 - 72a_5 + \frac{11\pi^2 \zeta_3}{8} - \frac{1195\zeta_3}{32} + \frac{609\zeta_5}{8} \right. \\
 & + \left. \frac{5119\pi^4}{7680} - \frac{1639\pi^2}{256} - \frac{1905}{512} + \frac{3\log^5(2)}{5} - 3\log^4(2) + 2\pi^2 \log^3(2) - 6\pi^2 \log^2(2) - \frac{13}{30} \pi^4 \log(2) + 11\pi^2 \log(2) \right) \\
 & + TC_{Fn_h} \left(-24a_4 - \frac{1273\zeta_3}{72} + \frac{93\pi^4}{640} - \frac{1553\pi^2}{576} + \frac{8135}{384} - \log^4(2) - 2\pi^2 \log^2(2) + 5\pi^2 \log(2) \right) \\
 & + \left(\frac{239\zeta_3}{72} + \frac{199\pi^4}{1920} + \frac{643\pi^2}{576} + \frac{4079}{384} \right) TC_{Fn_l} + C_A C_F \left(\frac{3\zeta_3}{8} + \frac{\pi^2}{12} - \frac{1111}{384} - \frac{1}{4} \pi^2 \log(2) \right) \\
 & + C_F^2 \left(-\frac{3\zeta_3}{4} - \frac{5\pi^2}{16} + \frac{7}{128} + \frac{1}{2} \pi^2 \log(2) \right) + \left(\frac{143}{96} - \frac{\pi^2}{6} \right) TC_{Fn_h} + \left(\frac{71}{96} + \frac{\pi^2}{12} \right) TC_{Fn_l}, \\
 z_m^{(3)} = & C_A C_F^2 \left(-\frac{4a_4}{3} - \frac{19\pi^2 \zeta_3}{16} - \frac{773\zeta_3}{96} + \frac{45\zeta_5}{16} + \frac{65\pi^4}{432} + \frac{509\pi^2}{576} + \frac{13189}{4608} - \frac{\log^4(2)}{18} - \frac{31}{36} \pi^2 \log^2(2) - \frac{31}{72} \pi^2 \log(2) \right) \\
 & + C_A^2 C_F \left(\frac{11a_4}{3} + \frac{51\pi^2 \zeta_3}{64} + \frac{1343\zeta_3}{288} - \frac{65\zeta_5}{32} - \frac{179\pi^4}{3456} - \frac{1955\pi^2}{3456} - \frac{1322545}{124416} + \frac{11\log^4(2)}{72} + \frac{11}{36} \pi^2 \log^2(2) \right. \\
 & - \left. \frac{115}{72} \pi^2 \log(2) \right) + Tn_h \left(C_A C_F \left(-\frac{4a_4}{3} + \frac{\pi^2 \zeta_3}{8} - \frac{109\zeta_3}{144} - \frac{5\zeta_5}{8} - \frac{43\pi^4}{1080} - \frac{449\pi^2}{144} + \frac{144959}{15552} - \frac{\log^4(2)}{18} \right. \right. \\
 & + \left. \frac{1}{18} \pi^2 \log^2(2) + \frac{32}{9} \pi^2 \log(2) \right) + C_F^2 \left(\frac{8a_4}{3} - \frac{53\zeta_3}{24} + \frac{91\pi^4}{2160} - \frac{85\pi^2}{108} + \frac{1067}{576} + \frac{\log^4(2)}{9} - \frac{1}{9} \pi^2 \log^2(2) \right. \\
 & + \left. \frac{8}{9} \pi^2 \log(2) \right) + Tn_l \left(C_A C_F \left(-\frac{4a_4}{3} + \frac{89\zeta_3}{144} + \frac{19\pi^4}{2160} + \frac{175\pi^2}{432} + \frac{70763}{15552} - \frac{\log^4(2)}{18} - \frac{1}{9} \pi^2 \log^2(2) + \frac{11}{18} \pi^2 \log(2) \right) \right. \\
 & + \left. C_F^2 \left(\frac{8a_4}{3} + \frac{55\zeta_3}{24} - \frac{119\pi^4}{2160} + \frac{13\pi^2}{18} + \frac{1283}{576} + \frac{\log^4(2)}{9} + \frac{2}{9} \pi^2 \log^2(2) - \frac{11}{9} \pi^2 \log(2) \right) \right) \\
 & + C_F^3 \left(-12a_4 - \frac{\pi^2 \zeta_3}{16} - \frac{81\zeta_3}{16} + \frac{5\zeta_5}{8} - \frac{\pi^4}{48} - \frac{613\pi^2}{192} - \frac{2969}{768} - \frac{\log^4(2)}{2} + \frac{1}{2} \pi^2 \log^2(2) + \frac{29}{4} \pi^2 \log(2) \right) \\
 & + \left(\frac{2\zeta_3}{9} + \frac{13\pi^2}{108} - \frac{5917}{3888} \right) T^2 C_{Fn_h n_l} + \left(\frac{11\zeta_3}{18} + \frac{4\pi^2}{135} - \frac{9481}{7776} \right) T^2 C_{Fn_h^2} + \left(-\frac{7\zeta_3}{18} - \frac{13\pi^2}{108} - \frac{2353}{7776} \right) T^2 C_{Fn_l^2} \\
 & + \epsilon \left\{ \left(-\frac{\zeta_3^2}{2} + \frac{21}{8} \pi^2 \log(2) \zeta_3 + \frac{1621\pi^2 \zeta_3}{192} - \frac{1761\zeta_3}{16} - 300a_4 + \frac{103\zeta_5}{4} - 72a_5 + \frac{3\log^5(2)}{5} + \frac{1}{8} \pi^2 \log^4(2) \right. \right. \\
 & - \left. \frac{25\log^4(2)}{2} - \pi^2 \log^3(2) - \frac{1}{8} \pi^4 \log^2(2) - \frac{93}{4} \pi^2 \log^2(2) - \frac{141}{160} \pi^4 \log(2) + \frac{317}{4} \pi^2 \log(2) - \frac{5\pi^6}{189} + \frac{437\pi^4}{1280} \right. \\
 & + \left. 3a_4 \pi^2 - \frac{110185\pi^2}{6144} - \frac{15709}{512} \right) C_F^3 + C_A \left(-\frac{249\zeta_3^2}{16} + 7\pi^2 \log(2) \zeta_3 - \frac{3125\pi^2 \zeta_3}{384} - \frac{767\zeta_3}{36} + \frac{34a_4}{9} + \frac{5935\zeta_5}{48} \right. \\
 & - \left. \frac{200a_5}{3} + \frac{5\log^5(2)}{9} + \frac{1}{3} \pi^2 \log^4(2) + \frac{17\log^4(2)}{108} + \frac{181}{54} \pi^2 \log^3(2) - \frac{1}{3} \pi^4 \log^2(2) - \frac{4765}{216} \pi^2 \log^2(2) + \frac{911\pi^4 \log(2)}{1728} \right. \\
 & - \left. \frac{1181}{54} \pi^2 \log(2) - \frac{7709\pi^6}{60480} + \frac{10219\pi^4}{3240} + 8a_4 \pi^2 - \frac{174769\pi^2}{55296} + \frac{339421}{27648} \right) C_F^2 \\
 & + n_l^2 T^2 \left(-\frac{197\zeta_3}{54} - \frac{23\pi^4}{270} - \frac{679\pi^2}{864} - \frac{131425}{46656} \right) C_F + n_h^2 T^2 \left(\frac{16a_4}{3} + \frac{1247\zeta_3}{270} + \frac{2\log^4(2)}{9} - \frac{2}{9} \pi^2 \log^2(2) \right)
 \end{aligned}$$

$$\begin{aligned}
 & -\frac{8}{45}\pi^2 \log(2) - \frac{31\pi^4}{1080} + \frac{5803\pi^2}{7200} - \frac{2404781}{233280} \Big) C_F + n_h n_l T^2 \left(\frac{16a_4}{3} + \frac{163\zeta_3}{27} + \frac{2\log^4(2)}{9} + \frac{4}{9}\pi^2 \log^2(2) - \frac{16}{9}\pi^2 \log(2) \right. \\
 & + \frac{5\pi^4}{72} + \frac{289\pi^2}{432} - \frac{314485}{23328} \Big) C_F + C_A^2 \left(\frac{137\zeta_3^2}{16} - \frac{133}{32}\pi^2 \log(2)\zeta_3 + \frac{43\pi^2\zeta_3}{48} + \frac{7433\zeta_3}{432} + \frac{658a_4}{9} - \frac{2939\zeta_5}{48} \right. \\
 & + \frac{154a_5}{3} - \frac{77\log^5(2)}{180} - \frac{19}{96}\pi^2 \log^4(2) + \frac{329\log^4(2)}{108} - \frac{77}{54}\pi^2 \log^3(2) + \frac{19}{96}\pi^4 \log^2(2) + \frac{1819}{108}\pi^2 \log^2(2) \\
 & - \frac{187\pi^4 \log(2)}{4320} - \frac{3835}{432}\pi^2 \log(2) + \frac{9469\pi^6}{120960} - \frac{31319\pi^4}{20736} - \frac{19a_4\pi^2}{4} - \frac{17873\pi^2}{6912} - \frac{52167985}{746496} \Big) C_F \\
 & + n_h T \left(\left(-\frac{328a_4}{9} - \frac{211\pi^2\zeta_3}{48} - \frac{499\zeta_3}{18} + \frac{28\zeta_5}{3} + 16a_5 - \frac{2\log^5(2)}{15} - \frac{41\log^4(2)}{27} + \frac{2}{9}\pi^2 \log^3(2) - \frac{175}{27}\pi^2 \log^2(2) \right. \right. \\
 & + \frac{29}{180}\pi^4 \log(2) + \frac{1151}{54}\pi^2 \log(2) + \frac{5393\pi^4}{12960} - \frac{136901\pi^2}{13824} + \frac{19129}{1152} \Big) C_F^2 + C_A \left(\frac{19\zeta_3^2}{8} + \frac{21}{8}\pi^2 \log(2)\zeta_3 \right. \\
 & + \frac{41\pi^2\zeta_3}{12} - \frac{44381\zeta_3}{432} - \frac{1228a_4}{9} - \frac{143\zeta_5}{12} - 8a_5 + \frac{\log^5(2)}{15} + \frac{1}{8}\pi^2 \log^4(2) - \frac{307\log^4(2)}{54} - \frac{1}{9}\pi^2 \log^3(2) \\
 & - \frac{1}{8}\pi^4 \log^2(2) - \frac{697}{27}\pi^2 \log^2(2) - \frac{29}{360}\pi^4 \log(2) + \frac{2147}{54}\pi^2 \log(2) - \frac{41\pi^6}{1080} + \frac{18151\pi^4}{25920} + 3a_4\pi^2 - \frac{8677\pi^2}{864} \\
 & + \frac{6253805}{93312} \Big) C_F \Big) + n_l T \left(\left(\frac{496a_4}{9} - \frac{73\pi^2\zeta_3}{48} + \frac{491\zeta_3}{18} - \frac{131\zeta_5}{3} + \frac{112a_5}{3} - \frac{14\log^5(2)}{45} + \frac{62\log^4(2)}{27} - \frac{28}{27}\pi^2 \log^3(2) \right. \right. \\
 & + \frac{124}{27}\pi^2 \log^2(2) - \frac{17}{540}\pi^4 \log(2) - \frac{256}{27}\pi^2 \log(2) - \frac{11527\pi^4}{25920} + \frac{89507\pi^2}{13824} + \frac{54083}{3456} \Big) C_F^2 \\
 & + C_A \left(-\frac{248a_4}{9} + \frac{13\pi^2\zeta_3}{24} + \frac{2329\zeta_3}{432} + \frac{455\zeta_5}{24} - \frac{56a_5}{3} + \frac{7\log^5(2)}{45} - \frac{31\log^4(2)}{27} + \frac{14}{27}\pi^2 \log^3(2) - \frac{62}{27}\pi^2 \log^2(2) \right. \\
 & \left. \left. + \frac{17\pi^4 \log(2)}{1080} + \frac{128}{27}\pi^2 \log(2) + \frac{11297\pi^4}{25920} + \frac{2587\pi^2}{864} + \frac{2963153}{93312} \right) C_F \right) \Big\},
 \end{aligned}$$

with

$$a_4 = \text{Li}_4\left(\frac{1}{2}\right).$$

The logarithmic contributions can be found in Appendix C.

APPENDIX C: RENORMALIZATION SCALE DEPENDENCE OF $z_m^{(4)}$

In this appendix we present the dependence of $z_m(\mu)$ and $c_m(\mu)$ on $\log(\mu)$. The corresponding analytic expressions are easily constructed from Eqs. (10) and (13) by taking the derivative with respect to μ^2 and exploiting the fact that M is μ independent. The μ dependence of $m(\mu)$ and $\alpha_s(\mu)$ is governed by corresponding renormalization group equations which are needed to four- and three-loop accuracy, respectively.

Our results read

$$z_m^{(1),\log} = -\frac{3}{4}C_F L_M, \tag{C1}$$

$$z_m^{(2),\log} = L_M \left(-\frac{185C_A C_F}{96} + \frac{13}{24}TC_F n_h + \frac{13}{24}TC_F n_l + \frac{21C_F^2}{32} \right) + L_M^2 \left\{ -\frac{11C_A C_F}{32} + \frac{1}{8}TC_F n_h + \frac{1}{8}TC_F n_l + \frac{9C_F^2}{32} \right\}, \tag{C2}$$

$$\begin{aligned}
z_m^{(3),\log} = & L_M \left\{ Tn_h \left(C_A C_F \left(\frac{\zeta_3}{2} + \frac{\pi^2 l_2}{6} - \frac{13\pi^2}{36} + \frac{583}{108} \right) + C_F^2 \left(-\frac{\zeta_3}{4} - \frac{1}{3}\pi^2 l_2 + \frac{\pi^2}{3} - \frac{151}{384} \right) \right) \right. \\
& + C_A C_F^2 \left(-\frac{53\zeta_3}{32} + \frac{53\pi^2 l_2}{48} - \frac{61\pi^2}{96} + \frac{5813}{1536} \right) + C_A^2 C_F \left(\frac{11\zeta_3}{16} - \frac{11}{24}\pi^2 l_2 + \frac{11\pi^2}{72} - \frac{13243}{1728} \right) \\
& + Tn_l \left(C_A C_F \left(\frac{\zeta_3}{2} + \frac{\pi^2 l_2}{6} + \frac{7\pi^2}{72} + \frac{869}{216} \right) + C_F^2 \left(-\frac{\zeta_3}{4} - \frac{1}{3}\pi^2 l_2 + \frac{7\pi^2}{48} + \frac{65}{384} \right) \right) + \left(\frac{\pi^2}{18} - \frac{143}{108} \right) T^2 C_F n_h n_l \\
& + \left. \left(\frac{\pi^2}{9} - \frac{197}{216} \right) T^2 C_F n_h^2 + C_F^3 \left(\frac{9\zeta_3}{16} - \frac{3}{8}\pi^2 l_2 + \frac{15\pi^2}{64} - \frac{489}{512} \right) + \left(-\frac{89}{216} - \frac{\pi^2}{18} \right) T^2 C_F n_l^2 \right\} \\
& + L_M^2 \left\{ Tn_h \left(\frac{373 C_A C_F}{288} - \frac{13 C_F^2}{32} \right) + Tn_l \left(\frac{373 C_A C_F}{288} - \frac{13 C_F^2}{32} \right) + \frac{109}{64} C_A C_F^2 - \frac{2341 C_A^2 C_F}{1152} - \frac{13}{36} T^2 C_F n_h n_l \right. \\
& - \left. \frac{13}{72} T^2 C_F n_h^2 - \frac{13}{72} T^2 C_F n_l^2 - \frac{27 C_F^3}{128} \right\} + L_M^3 \left\{ Tn_h \left(\frac{11 C_A C_F}{72} - \frac{3 C_F^2}{32} \right) + Tn_l \left(\frac{11 C_A C_F}{72} - \frac{3 C_F^2}{32} \right) + \frac{33}{128} C_A C_F^2 \right. \\
& - \left. \frac{121}{576} C_A^2 C_F - \frac{1}{18} T^2 C_F n_h n_l - \frac{1}{36} T^2 C_F n_h^2 - \frac{1}{36} T^2 C_F n_l^2 - \frac{9 C_F^3}{128} \right\}, \tag{C3}
\end{aligned}$$

$$\begin{aligned}
z_m^{(4),\log} = & L_M \left\{ \left(\frac{3l_2^4}{8} - \frac{3}{8}\pi^2 l_2^2 - \frac{351\pi^2 l_2}{64} + 9a_4 + \frac{3\pi^2 \zeta_3}{64} + \frac{663\zeta_3}{128} - \frac{15\zeta_5}{32} + \frac{\pi^4}{64} + \frac{1241\pi^2}{512} + \frac{18505}{4096} \right) C_F^4 \right. \\
& + C_A \left(-\frac{4l_2^4}{3} + \frac{97}{48}\pi^2 l_2^2 + \frac{7595\pi^2 l_2}{384} - 32a_4 + \frac{23\pi^2 \zeta_3}{32} - \frac{2149\zeta_3}{256} - \frac{25\zeta_5}{64} - \frac{49\pi^4}{288} - \frac{4677\pi^2}{512} - \frac{55487}{3072} \right) C_F^3 \\
& + C_A^2 \left(-\frac{77l_2^4}{288} - \frac{187}{72}\pi^2 l_2^2 + \frac{1123\pi^2 l_2}{1152} - \frac{77a_4}{12} - \frac{989\pi^2 \zeta_3}{256} - \frac{6781\zeta_3}{256} + \frac{965\zeta_5}{128} + \frac{6257\pi^4}{13824} \right. \\
& + \left. \frac{3575\pi^2}{1536} + \frac{8025563}{331776} \right) C_F^2 + \frac{2489n_h n_l^2 T^3 C_F}{1296} + n_h^2 n_l T^3 \left(-\zeta_3 - \frac{3\pi^2}{20} + \frac{3677}{1296} \right) C_F \\
& + n_h^3 T^3 \left(-\frac{2\zeta_3}{3} - \frac{4\pi^2}{135} + \frac{4865}{3888} \right) C_F + n_l^3 T^3 \left(\frac{\zeta_3}{3} + \frac{13\pi^2}{108} + \frac{1301}{3888} \right) C_F + C_A^3 \left(\frac{121l_2^4}{288} + \frac{121}{144}\pi^2 l_2^2 \right. \\
& - \left. \frac{1367\pi^2 l_2}{288} + \frac{121a_4}{12} + \frac{561\pi^2 \zeta_3}{256} + \frac{1223\zeta_3}{96} - \frac{495\zeta_5}{128} - \frac{1969\pi^4}{13824} - \frac{19873\pi^2}{13824} - \frac{4722671}{124416} \right) C_F - \frac{d_{FF} n_h}{4N_c} \\
& - \frac{d_{FF} n_l}{4N_c} + \frac{15d_{FF} n_h \zeta_3}{8N_c} + \frac{15d_{FF} n_l \zeta_3}{8N_c} - \frac{15d_{FA} \zeta_3}{16N_c} + \frac{d_{FA}}{8N_c} + n_l^2 T^2 \left(\left(-\frac{l_2^4}{9} - \frac{2}{9}\pi^2 l_2^2 + \frac{11\pi^2 l_2}{9} - \frac{8a_4}{3} - \frac{11\zeta_3}{8} \right. \right. \\
& + \left. \left. \frac{11\pi^4}{216} - \frac{21\pi^2}{32} - \frac{50131}{20736} \right) C_F^2 + C_A \left(\frac{l_2^4}{18} + \frac{1}{9}\pi^2 l_2^2 - \frac{11\pi^2 l_2}{18} + \frac{4a_4}{3} - \frac{37\zeta_3}{16} - \frac{\pi^4}{216} - \frac{29\pi^2}{36} - \frac{15953}{2592} \right) C_F \right) \\
& + n_h n_l T^2 \left(\left(-\frac{2l_2^4}{9} - \frac{1}{9}\pi^2 l_2^2 + \frac{\pi^2 l_2}{3} - \frac{16a_4}{3} + \zeta_3 + \frac{\pi^4}{216} - \frac{\pi^2}{864} - \frac{41383}{10368} \right) C_F^2 + C_A \left(\frac{l_2^4}{9} + \frac{1}{18}\pi^2 l_2^2 \right. \right. \\
& - \left. \left. \frac{25\pi^2 l_2}{6} + \frac{8a_4}{3} - \frac{\pi^2 \zeta_3}{8} - \frac{\zeta_3}{2} + \frac{5\zeta_5}{8} + \frac{17\pi^4}{432} + \frac{1345\pi^2}{432} - \frac{26213}{1296} \right) C_F \right) + n_h^2 T^2 \left(\left(-\frac{l_2^4}{9} + \frac{1}{9}\pi^2 l_2^2 - \frac{8\pi^2 l_2}{9} \right. \right. \\
& - \left. \left. \frac{8a_4}{3} + \frac{19\zeta_3}{8} - \frac{5\pi^4}{108} + \frac{1757\pi^2}{2160} - \frac{32635}{20736} \right) C_F^2 + C_A \left(\frac{l_2^4}{18} - \frac{1}{18}\pi^2 l_2^2 - \frac{32\pi^2 l_2}{9} + \frac{4a_4}{3} - \frac{\pi^2 \zeta_3}{8} + \frac{29\zeta_3}{16} + \frac{5\zeta_5}{8} \right. \right. \\
& + \left. \left. \frac{19\pi^4}{432} + \frac{7211\pi^2}{2160} - \frac{36473}{2592} \right) C_F \right) + n_l T \left(\left(\frac{5l_2^4}{12} - \frac{2}{3}\pi^2 l_2^2 - \frac{311\pi^2 l_2}{48} + 10a_4 + \frac{\pi^2 \zeta_3}{16} + \frac{69\zeta_3}{32} + \frac{5\zeta_5}{4} + \frac{179\pi^4}{2880} \right. \right. \\
& + \left. \left. \frac{175\pi^2}{64} + \frac{883}{512} \right) C_F^3 + C_A \left(\frac{29l_2^4}{72} + \frac{14}{9}\pi^2 l_2^2 - \frac{1075\pi^2 l_2}{288} + \frac{29a_4}{3} + \frac{19\pi^2 \zeta_3}{16} + \frac{391\zeta_3}{32} - \frac{25\zeta_5}{8} - \frac{2567\pi^4}{8640} \right. \right.
\end{aligned}$$

$$\begin{aligned}
 & + \frac{365\pi^2}{384} + \frac{12563}{10368} \Big) C_F^2 + C_A^2 \left(-\frac{11l_2^4}{36} - \frac{11}{18}\pi^2 l_2^2 + \frac{251\pi^2 l_2}{72} - \frac{22a_4}{3} - \frac{51\pi^2 \zeta_3}{64} + \frac{7\zeta_3}{32} + \frac{15\zeta_5}{32} + \frac{223\pi^4}{3456} \right. \\
 & + \frac{1991\pi^2}{1152} + \frac{601319}{20736} \Big) C_F \Big) + n_h T \left(\left(\frac{5l_2^4}{12} - \frac{5}{12}\pi^2 l_2^2 - \frac{129\pi^2 l_2}{16} + 10a_4 + \frac{\pi^2 \zeta_3}{16} + \frac{177\zeta_3}{32} + \frac{5\zeta_5}{4} - \frac{31\pi^4}{2880} \right. \right. \\
 & + \frac{4481\pi^2}{1152} + \frac{991}{512} \Big) C_F^3 + C_A \left(\frac{29l_2^4}{72} + \frac{37}{72}\pi^2 l_2^2 - \frac{13\pi^2 l_2}{96} + \frac{29a_4}{3} + \frac{35\pi^2 \zeta_3}{32} + \frac{7\zeta_3}{8} - \frac{85\zeta_5}{32} + \frac{29\pi^4}{4320} \right. \\
 & - \frac{527\pi^2}{1728} - \frac{10771}{2592} \Big) C_F^2 + C_A^2 \left(-\frac{11l_2^4}{36} - \frac{11}{72}\pi^2 l_2^2 + \frac{139\pi^2 l_2}{12} - \frac{22a_4}{3} - \frac{29\pi^2 \zeta_3}{64} - \frac{57\zeta_3}{16} - \frac{5\zeta_5}{4} - \frac{239\pi^4}{3456} \right. \\
 & - \frac{28735\pi^2}{3456} + \frac{895403}{20736} \Big) C_F \Big) \Big\} + L_M^2 \left\{ T^2 n_h^2 \left(C_A C_F \left(-\frac{\zeta_3}{4} - \frac{1}{12}\pi^2 l_2 + \frac{\pi^2}{3} - \frac{9707}{2304} \right) \right. \right. \\
 & + C_F^2 \left(\frac{\zeta_3}{8} + \frac{\pi^2 l_2}{6} - \frac{5\pi^2}{24} + \frac{923}{2304} \right) \Big) + T^2 n_h n_l \left(C_A C_F \left(-\frac{\zeta_3}{2} - \frac{1}{6}\pi^2 l_2 + \frac{5\pi^2}{24} - \frac{8123}{1152} \right) \right. \\
 & + C_F^2 \left(\frac{\zeta_3}{4} + \frac{\pi^2 l_2}{3} - \frac{25\pi^2}{96} + \frac{383}{1152} \right) \Big) + T n_h \left(C_A C_F^2 \left(\frac{\zeta_3}{64} - \frac{103}{96}\pi^2 l_2 + \frac{175\pi^2}{192} - \frac{10853}{2304} \right) \right. \\
 & + C_A^2 C_F \left(\frac{11\zeta_3}{32} + \frac{11\pi^2 l_2}{24} - \frac{55\pi^2}{96} + \frac{6527}{512} \right) + C_F^3 \left(\frac{3\zeta_3}{32} + \frac{5\pi^2 l_2}{16} - \frac{31\pi^2}{128} + \frac{57}{256} \right) \Big) \\
 & + C_A C_F^3 \left(\frac{357\zeta_3}{256} - \frac{119}{128}\pi^2 l_2 + \frac{287\pi^2}{512} - \frac{6477}{2048} \right) + C_A^2 C_F^2 \left(-\frac{649\zeta_3}{256} + \frac{649\pi^2 l_2}{384} - \frac{715\pi^2}{768} + \frac{373625}{36864} \right) \\
 & + C_A^3 C_F \left(\frac{121\zeta_3}{128} - \frac{121}{192}\pi^2 l_2 + \frac{121\pi^2}{576} - \frac{337657}{27648} \right) + T^2 n_l^2 \left(C_A C_F \left(-\frac{\zeta_3}{4} - \frac{1}{12}\pi^2 l_2 - \frac{\pi^2}{8} - \frac{6539}{2304} \right) \right. \\
 & + C_F^2 \left(\frac{\zeta_3}{8} + \frac{\pi^2 l_2}{6} - \frac{5\pi^2}{96} - \frac{157}{2304} \right) \Big) + T n_l \left(C_A C_F^2 \left(\frac{\zeta_3}{64} - \frac{103}{96}\pi^2 l_2 + \frac{185\pi^2}{384} - \frac{7883}{2304} \right) \right. \\
 & + C_A^2 C_F \left(\frac{11\zeta_3}{32} + \frac{11\pi^2 l_2}{24} + \frac{11\pi^2}{192} + \frac{5559}{512} \right) + C_F^3 \left(\frac{3\zeta_3}{32} + \frac{5\pi^2 l_2}{16} - \frac{11\pi^2}{64} + \frac{3}{256} \right) \Big) + \frac{125}{144} T^3 C_F n_h n_l^2 \\
 & + \left(\frac{161}{144} - \frac{\pi^2}{12} \right) T^3 C_F n_h^2 n_l + \left(\frac{197}{432} - \frac{\pi^2}{18} \right) T^3 C_F n_h^3 + C_F^4 \left(-\frac{27\zeta_3}{128} + \frac{9\pi^2 l_2}{64} - \frac{45\pi^2}{512} + \frac{2889}{4096} \right) \\
 & + \left(\frac{89}{432} + \frac{\pi^2}{36} \right) T^3 C_F n_l^3 \Big\} + L_M^3 \left\{ T^2 n_h n_l \left(\frac{97C_F^2}{288} - \frac{91C_A C_F}{72} \right) + T^2 n_h^2 \left(\frac{97C_F^2}{576} - \frac{91C_A C_F}{144} \right) \right. \\
 & + T n_h \left(-\frac{389}{288} C_A C_F^2 + \frac{1163}{576} C_A^2 C_F + \frac{9C_F^3}{64} \right) + T^2 n_l^2 \left(\frac{97C_F^2}{576} - \frac{91C_A C_F}{144} \right) + T n_l \left(-\frac{389}{288} C_A C_F^2 \right. \\
 & + \frac{1163}{576} C_A^2 C_F + \frac{9C_F^3}{64} \Big) - \frac{45}{64} C_A C_F^3 + \frac{21361C_A^2 C_F^2}{9216} - \frac{27995C_A^3 C_F}{13824} + \frac{13}{72} T^3 C_F n_h n_l^2 + \frac{13}{72} T^3 C_F n_h^2 n_l + \frac{13}{216} T^3 C_F n_h^3 \\
 & + \frac{13}{216} T^3 C_F n_l^3 + \frac{45C_F^4}{1024} \Big\} + L_M^4 \left\{ T^2 n_h n_l \left(\frac{11C_F^2}{192} - \frac{11C_A C_F}{96} \right) + T^2 n_h^2 \left(\frac{11C_F^2}{384} - \frac{11C_A C_F}{192} \right) \right. \\
 & + T n_h \left(-\frac{121}{768} C_A C_F^2 + \frac{121}{768} C_A^2 C_F + \frac{9C_F^3}{256} \right) + T^2 n_l^2 \left(\frac{11C_F^2}{384} - \frac{11C_A C_F}{192} \right) + T n_l \left(-\frac{121}{768} C_A C_F^2 + \frac{121}{768} C_A^2 C_F + \frac{9C_F^3}{256} \right) \\
 & - \frac{99C_A C_F^3}{1024} + \frac{1331C_A^2 C_F^2}{6144} - \frac{1331C_A^3 C_F}{9216} + \frac{1}{48} T^3 C_F n_h n_l^2 + \frac{1}{48} T^3 C_F n_h^2 n_l + \frac{1}{144} T^3 C_F n_h^3 + \frac{1}{144} T^3 C_F n_l^3 + \frac{27C_F^4}{2048} \Big\}, \\
 & \tag{C4}
 \end{aligned}$$

with

$$d_{FF} = d_F^{abcd} d_F^{abcd}, \quad d_{FA} = d_F^{abcd} d_A^{abcd}, \quad L_M = \log\left(\frac{\mu^2}{M^2}\right), \quad l_2 = \log(2). \quad (C5)$$

We present the μ dependence of the four-loop term of the inverted relation in the form

$$c_m^{(4),\log} = -z_m^{(4),\log}|_{L_M \rightarrow l_m} + \delta c_m^{(4),\log}, \quad (C6)$$

where

$$\begin{aligned} \delta c_m^{(4),\log} = & l_m \left(T n_h \left(C_A C_F^2 \left(2a_4 - \frac{3\pi^2 \zeta_3}{16} + \frac{89\zeta_3}{48} + \frac{15\zeta_5}{16} + \frac{l_2^4}{12} - \frac{1}{12} \pi^2 l_2^2 - \frac{85\pi^2 l_2}{16} + \frac{43\pi^4}{720} + \frac{43\pi^2}{9} - \frac{95551}{20736} \right) \right. \right. \\ & + C_F^3 \left(-4a_4 + \frac{21\zeta_3}{8} - \frac{l_2^4}{6} + \frac{1}{6} \pi^2 l_2^2 - \frac{11\pi^2 l_2}{8} - \frac{91\pi^4}{1440} + \frac{641\pi^2}{576} - \frac{917}{384} \right) \left. \right) + C_A C_F^3 \left(2a_4 + \frac{57\pi^2 \zeta_3}{32} + \frac{1635\zeta_3}{128} \right. \\ & - \frac{135\zeta_5}{32} + \frac{l_2^4}{12} + \frac{31}{24} \pi^2 l_2^2 + \frac{35\pi^2 l_2}{192} - \frac{65\pi^4}{288} - \frac{827\pi^2}{768} + \frac{191}{3072} \left. \right) + C_A^2 C_F^2 \left(-\frac{11a_4}{2} - \frac{153\pi^2 \zeta_3}{128} - \frac{2779\zeta_3}{384} + \frac{195\zeta_5}{64} \right. \\ & - \frac{11l_2^4}{48} - \frac{11}{24} \pi^2 l_2^2 + \frac{491\pi^2 l_2}{192} + \frac{179\pi^4}{2304} + \frac{1831\pi^2}{2304} - \frac{16873}{165888} \left. \right) + T n_l \left(C_A C_F^2 \left(2a_4 - \frac{5\zeta_3}{24} + \frac{l_2^4}{12} + \frac{1}{6} \pi^2 l_2^2 - \frac{43\pi^2 l_2}{48} \right. \right. \\ & - \frac{19\pi^4}{1440} - \frac{385\pi^2}{576} + \frac{62885}{20736} \left. \right) + C_F^3 \left(-4a_4 - \frac{33\zeta_3}{8} - \frac{l_2^4}{6} - \frac{1}{3} \pi^2 l_2^2 + \frac{43\pi^2 l_2}{24} + \frac{119\pi^4}{1440} - \frac{97\pi^2}{96} - \frac{1295}{384} \right) \left. \right) \\ & + C_F^4 \left(18a_4 + \frac{3\pi^2 \zeta_3}{32} + \frac{459\zeta_3}{64} - \frac{15\zeta_5}{16} + \frac{3l_2^4}{4} - \frac{3}{4} \pi^2 l_2^2 - \frac{339\pi^2 l_2}{32} + \frac{\pi^4}{32} + \frac{1181\pi^2}{256} + \frac{11135}{2048} \right) \\ & + \left(-\frac{\zeta_3}{3} - \frac{25\pi^2}{144} - \frac{1861}{5184} \right) T^2 C_F^2 n_h n_l + \left(-\frac{11\zeta_3}{12} - \frac{11\pi^2}{360} + \frac{4943}{10368} \right) T^2 C_F^2 n_h^2 + \left(\frac{7\zeta_3}{12} + \frac{25\pi^2}{144} - \frac{8665}{10368} \right) T^2 C_F^2 n_l^2 \\ & + l_m^2 \left(T n_h \left(C_A C_F^2 \left(-\frac{21\zeta_3}{32} - \frac{5}{16} \pi^2 l_2 + \frac{65\pi^2}{96} - \frac{751}{144} \right) + C_F^3 \left(\frac{3\zeta_3}{16} + \frac{5\pi^2 l_2}{8} - \frac{25\pi^2}{64} - \frac{237}{512} \right) \right) \right. \\ & + C_A C_F^3 \left(\frac{165\zeta_3}{64} - \frac{55}{32} \pi^2 l_2 + \frac{275\pi^2}{256} - \frac{8661}{2048} \right) + C_A^2 C_F^2 \left(-\frac{165\zeta_3}{128} + \frac{55\pi^2 l_2}{64} - \frac{55\pi^2}{192} + \frac{126869}{18432} \right) \\ & + T n_l \left(C_A C_F^2 \left(-\frac{21\zeta_3}{32} - \frac{5}{16} \pi^2 l_2 - \frac{35\pi^2}{192} - \frac{1519}{576} \right) + C_F^3 \left(\frac{3\zeta_3}{16} + \frac{5\pi^2 l_2}{8} - \frac{25\pi^2}{64} - \frac{237}{512} \right) \right) \\ & + \left(\frac{623}{576} - \frac{5\pi^2}{48} \right) T^2 C_F^2 n_h n_l + \left(\frac{1163}{1152} - \frac{5\pi^2}{24} \right) T^2 C_F^2 n_h^2 + \left(\frac{83}{1152} + \frac{5\pi^2}{48} \right) T^2 C_F^2 n_l^2 + \frac{2169 C_F^4}{1024} \\ & + l_m^3 \left(T n_h \left(\frac{45 C_F^3}{128} - \frac{1061}{576} C_A C_F^2 \right) + T n_l \left(\frac{45 C_F^3}{128} - \frac{1061}{576} C_A C_F^2 \right) - \frac{693}{512} C_A C_F^3 + \frac{14101 C_A^2 C_F^2}{4608} + \frac{67}{144} T^2 C_F^2 n_h n_l \right. \\ & + \frac{67}{288} T^2 C_F^2 n_h^2 + \frac{67}{288} T^2 C_F^2 n_l^2 - \frac{45 C_F^4}{256} \left. \right) + l_m^4 \left(-\frac{121}{384} T C_A C_F^2 n_h - \frac{121}{384} T C_A C_F^2 n_l + \frac{1331 C_A^2 C_F^2}{3072} + \frac{11}{96} T^2 C_F^2 n_h n_l \right. \\ & \left. + \frac{11}{192} T^2 C_F^2 n_h^2 + \frac{11}{192} T^2 C_F^2 n_l^2 + \frac{27 C_F^4}{1024} \right), \quad (C7) \end{aligned}$$

with

$$l_m = \log\left(\frac{\mu^2}{m^2(\mu)}\right). \quad (C8)$$

Note that the μ dependence at four-loop order has also been discussed in Ref. [78].

APPENDIX D: COUNTERTERM CONTRIBUTION TO Z_m^{OS}

In this Appendix we show the four-loop contribution to Z_m^{OS} introduced by the lower loop orders. To be precise we write

$$Z_m^{\text{OS}} = \sum_{n \geq 0} \left(\frac{\alpha_s(\mu)}{\pi} \right)^n Z_m^{\text{OS},(n)} \quad (\text{D1})$$

and split $Z_m^{\text{OS},(4)}$ according to

$$Z_m^{\text{OS},(4)} = Z_m^{\text{OS},(4)}|_{\text{CT}} + Z_m^{\text{OS},(4)}|_{\text{genuine 4 loop}}, \quad (\text{D2})$$

where $Z_m^{\text{OS},(4)}|_{\text{CT}}$ contains all counterterm contributions from the renormalization of the strong coupling constant and quark mass. For $\mu^2 = M^2$ it is given by

$$\begin{aligned} Z_m^{\text{OS},(4)}|_{\text{CT}} = & \left\{ T^2 n_h n_l \left(\frac{11 C_A C_F}{48} + \frac{17 C_F^2}{64} \right) + T^2 n_h^2 \left(\frac{11 C_A C_F}{96} + \frac{11 C_F^2}{64} \right) + T n_h \left(-\frac{47}{64} C_A C_F^2 - \frac{121}{384} C_A^2 C_F - \frac{189 C_F^3}{256} \right) \right. \\ & + T^2 n_l^2 \left(\frac{11 C_A C_F}{96} + \frac{11 C_F^2}{96} \right) + T n_l \left(-\frac{121}{192} C_A C_F^2 - \frac{121}{384} C_A^2 C_F - \frac{135 C_F^3}{256} \right) + \frac{1377 C_A C_F^3}{1024} + \frac{1331 C_A^2 C_F^2}{1536} \\ & + \frac{1331 C_A^3 C_F}{4608} - \frac{1}{24} T^3 C_F n_h n_l^2 - \frac{1}{24} T^3 C_F n_h^2 n_l - \frac{1}{72} T^3 C_F n_h^3 - \frac{1}{72} T^3 C_F n_l^3 + \frac{243 C_F^4}{256} \left. \right\} \frac{1}{\epsilon^4} \\ & + \left\{ T^2 n_h n_l \left(\frac{235 C_A C_F}{288} + \frac{337 C_F^2}{384} \right) + T^2 n_h^2 \left(\frac{235 C_A C_F}{576} + \frac{175 C_F^2}{384} \right) + T n_h \left(-\frac{1399}{512} C_A C_F^2 - \frac{2671 C_A^2 C_F}{2304} \right. \right. \\ & - \left. \frac{559 C_F^3}{512} \right) + T^2 n_l^2 \left(\frac{235 C_A C_F}{576} + \frac{27 C_F^2}{64} \right) + T n_l \left(-\frac{325}{128} C_A C_F^2 - \frac{2671 C_A^2 C_F}{2304} - \frac{5 C_F^3}{4} \right) \\ & + \frac{1}{256} (904 - 3\pi^2) C_A C_F^3 + \frac{3841 C_A^2 C_F^2}{1024} + \frac{3421 C_A^3 C_F}{3072} - \frac{7}{48} T^3 C_F n_h n_l^2 - \frac{7}{48} T^3 C_F n_h^2 n_l - \frac{7}{144} T^3 C_F n_h^3 \\ & - \left. \frac{7}{144} T^3 C_F n_l^3 - \frac{45 C_F^4}{512} \right\} \frac{1}{\epsilon^3} + \left\{ T n_h \left(C_A C_F^2 \left(-\frac{5\zeta_3}{16} + \frac{7\pi^2 l_2}{24} + \frac{157\pi^2}{256} - \frac{183953}{9216} \right) \right. \right. \\ & + \left. \left(-\frac{11}{24} \pi^2 l_2 + \frac{1199\pi^2}{2304} - \frac{59435}{4608} \right) C_A^2 C_F + C_F^3 \left(-\frac{21\zeta_3}{16} + \frac{5\pi^2 l_2}{4} - \frac{59\pi^2}{256} - \frac{35327}{3072} \right) \right) \\ & + T^2 n_h^2 \left(C_A C_F \left(\frac{\zeta_3}{8} + \frac{\pi^2 l_2}{12} - \frac{181\pi^2}{576} + \frac{7933}{1728} \right) + \left(-\frac{1}{6} \pi^2 l_2 - \frac{101\pi^2}{384} + \frac{10775}{2304} \right) C_F^2 \right) \\ & + T^2 n_h n_l \left(C_A C_F \left(\frac{\zeta_3}{4} + \frac{\pi^2 l_2}{6} - \frac{49\pi^2}{288} + \frac{6745}{864} \right) + \left(-\frac{1}{3} \pi^2 l_2 + \frac{\pi^2}{24} + \frac{15769}{2304} \right) C_F^2 \right) \\ & + C_A C_F^3 \left(\frac{1353\zeta_3}{512} - \frac{467}{256} \pi^2 l_2 + \frac{4149\pi^2}{2048} + \frac{20165}{1536} \right) + C_A^2 C_F^2 \left(-\frac{277\zeta_3}{512} + \frac{143\pi^2 l_2}{384} + \frac{\pi^4}{1440} \right. \\ & + \left. \frac{4103\pi^2}{18432} + \frac{122785}{6144} \right) + C_A^3 C_F \left(-\frac{121\zeta_3}{128} + \frac{121\pi^2 l_2}{192} - \frac{4477\pi^2}{27648} + \frac{1953781}{165888} \right) \\ & + T n_l \left(C_A C_F^2 \left(-\frac{35\zeta_3}{64} + \frac{31\pi^2 l_2}{96} - \frac{1963\pi^2}{2304} - \frac{10477}{768} \right) + \left(-\frac{11}{24} \pi^2 l_2 - \frac{253\pi^2}{2304} - \frac{50723}{4608} \right) C_A^2 C_F \right. \\ & + \left. C_F^3 \left(-\frac{33\zeta_3}{32} + \frac{19\pi^2 l_2}{16} - \frac{683\pi^2}{512} - \frac{4391}{768} \right) \right) + T^2 n_l^2 \left(C_A C_F \left(\frac{\zeta_3}{8} + \frac{\pi^2 l_2}{12} + \frac{83\pi^2}{576} + \frac{5557}{1728} \right) \right. \\ & + \left. \left(-\frac{1}{6} \pi^2 l_2 + \frac{323\pi^2}{1152} + \frac{871}{384} \right) C_F^2 \right) + \left(\frac{11\pi^2}{144} - \frac{1193}{864} \right) T^3 C_F n_h^2 n_l + \left(-\frac{977}{864} - \frac{\pi^2}{144} \right) T^3 C_F n_h n_l^2 \end{aligned}$$

$$\begin{aligned}
 & + \left(\frac{23\pi^2}{432} - \frac{1409}{2592} \right) T^3 C_F n_h^3 + C_F^4 \left(\frac{1107\zeta_3}{256} - \frac{369}{128} \pi^2 l_2 + \frac{297\pi^2}{128} + \frac{2787}{1024} \right) + \left(-\frac{761}{2592} - \frac{13\pi^2}{432} \right) T^3 C_F n_l^3 \left. \right\} \frac{1}{\epsilon^2} \\
 & + \left\{ \left(\frac{625l_2^4}{128} + \frac{225}{64} \pi^2 l_2^2 - \frac{745\pi^2 l_2}{16} + \frac{1875a_4}{16} + \frac{3\pi^2 \zeta_3}{64} + \frac{4695\zeta_3}{64} - \frac{75\zeta_5}{64} - \frac{2311\pi^4}{2560} + \frac{65941\pi^2}{3072} + \frac{44617}{2048} \right) C_F^4 \right. \\
 & + C_A \left(\frac{2557l_2^4}{768} + \frac{2341}{384} \pi^2 l_2^2 - \frac{1775\pi^2 l_2}{64} + \frac{2557a_4}{32} + \frac{317\pi^2 \zeta_3}{64} + \frac{39451\zeta_3}{512} - \frac{475\zeta_5}{32} - \frac{56531\pi^4}{46080} \right. \\
 & + \frac{169661\pi^2}{12288} + \frac{169787}{3072} \left. \right) C_F^3 + C_A^2 \left(-\frac{113l_2^4}{144} + \frac{79}{288} \pi^2 l_2^2 + \frac{10145\pi^2 l_2}{1152} - \frac{113a_4}{6} + \frac{115\pi^2 \zeta_3}{768} - \frac{2123\zeta_3}{4608} \right. \\
 & + \frac{187\zeta_5}{128} - \frac{5039\pi^4}{92160} + \frac{27593\pi^2}{12288} + \frac{3298805}{36864} \left. \right) C_F^2 + n_l^3 T^3 \left(-\frac{77\zeta_3}{108} - \frac{611\pi^2}{2592} - \frac{22697}{15552} \right) C_F \\
 & + n_h n_l^2 T^3 \left(-\frac{1}{3} \pi^2 l_2 + \frac{13\zeta_3}{36} + \frac{25\pi^2}{864} - \frac{32417}{5184} \right) C_F + n_h^3 T^3 \left(-\frac{1}{3} \pi^2 l_2 + \frac{193\zeta_3}{108} + \frac{3749\pi^2}{12960} - \frac{51857}{15552} \right) C_F \\
 & + n_h^2 n_l T^3 \left(-\frac{2}{3} \pi^2 l_2 + \frac{103\zeta_3}{36} + \frac{2393\pi^2}{4320} - \frac{42137}{5184} \right) C_F + C_A^3 \left(-\frac{605l_2^4}{576} - \frac{605}{288} \pi^2 l_2^2 + \frac{2405\pi^2 l_2}{288} - \frac{605a_4}{24} \right. \\
 & - \frac{561\pi^2 \zeta_3}{256} - \frac{148433\zeta_3}{6912} + \frac{715\zeta_5}{128} + \frac{25091\pi^4}{69120} + \frac{169519\pi^2}{165888} + \frac{64234201}{995328} \left. \right) C_F + n_l^2 T^2 \left(\left(\frac{5l_2^4}{18} + \frac{5}{9} \pi^2 l_2^2 - \frac{20\pi^2 l_2}{9} \right. \right. \\
 & + \frac{20a_4}{3} + \frac{2257\zeta_3}{288} - \frac{49\pi^4}{432} + \frac{5509\pi^2}{2304} + \frac{77327}{6912} \left. \right) C_F^2 + C_A \left(-\frac{5l_2^4}{36} - \frac{5}{18} \pi^2 l_2^2 + \frac{10\pi^2 l_2}{9} - \frac{10a_4}{3} + \frac{85\zeta_3}{36} + \frac{41\pi^4}{1080} \right. \\
 & + \frac{4655\pi^2}{3456} + \frac{343919}{20736} \left. \right) C_F \left. \right) + n_h^2 T^2 \left(\left(\frac{5l_2^4}{18} + \frac{2}{9} \pi^2 l_2^2 + \frac{43\pi^2 l_2}{18} + \frac{20a_4}{3} - \frac{369\zeta_3}{32} - \frac{7\pi^4}{432} - \frac{79751\pi^2}{34560} + \frac{109217}{4608} \right) C_F^2 \right. \\
 & + C_A \left(-\frac{5l_2^4}{36} - \frac{1}{9} \pi^2 l_2^2 + \frac{53\pi^2 l_2}{9} - \frac{10a_4}{3} + \frac{\pi^2 \zeta_3}{8} - \frac{721\zeta_3}{72} - \frac{5\zeta_5}{8} - \frac{23\pi^4}{2160} - \frac{27391\pi^2}{5760} + \frac{610895}{20736} \right) C_F \left. \right) \\
 & + n_h n_l T^2 \left(\left(\frac{5l_2^4}{9} + \frac{7}{9} \pi^2 l_2^2 + \frac{\pi^2 l_2}{24} + \frac{40a_4}{3} - \frac{79\zeta_3}{48} - \frac{7\pi^4}{54} - \frac{143\pi^2}{216} + \frac{475145}{13824} \right) C_F^2 \right. \\
 & + C_A \left(-\frac{5l_2^4}{18} - \frac{7}{18} \pi^2 l_2^2 + 7\pi^2 l_2 - \frac{20a_4}{3} + \frac{\pi^2 \zeta_3}{8} - \frac{551\zeta_3}{72} - \frac{5\zeta_5}{8} + \frac{59\pi^4}{2160} - \frac{6893\pi^2}{1728} + \frac{477407}{10368} \right) C_F \left. \right) \\
 & + n_l T \left(\left(-\frac{101l_2^4}{48} - \frac{65}{24} \pi^2 l_2^2 + \frac{155\pi^2 l_2}{8} - \frac{101a_4}{2} - \frac{\pi^2 \zeta_3}{16} - \frac{5045\zeta_3}{128} + \frac{5\zeta_5}{8} + \frac{1723\pi^4}{2880} - \frac{11719\pi^2}{1024} - \frac{15091}{512} \right) C_F^3 \right. \\
 & + C_A \left(-\frac{137l_2^4}{288} - \frac{245}{144} \pi^2 l_2^2 + \frac{371\pi^2 l_2}{144} - \frac{137a_4}{12} - \frac{19\pi^2 \zeta_3}{16} - \frac{1831\zeta_3}{72} + \frac{45\zeta_5}{16} + \frac{6601\pi^4}{17280} - \frac{15377\pi^2}{2304} - \frac{438589}{6912} \right) C_F^2 \\
 & + C_A^2 \left(\frac{55l_2^4}{72} + \frac{55}{36} \pi^2 l_2^2 - \frac{883\pi^2 l_2}{144} + \frac{55a_4}{3} + \frac{51\pi^2 \zeta_3}{64} + \frac{1949\zeta_3}{288} - \frac{65\zeta_5}{32} - \frac{817\pi^4}{3456} - \frac{10337\pi^2}{4608} - \frac{1610957}{27648} \right) C_F \left. \right) \\
 & + n_h T \left(\left(-\frac{19l_2^4}{8} - \frac{11}{8} \pi^2 l_2^2 + \frac{4679\pi^2 l_2}{768} - 57a_4 - \frac{\pi^2 \zeta_3}{16} - \frac{5777\zeta_3}{1536} + \frac{5\zeta_5}{8} + \frac{139\pi^4}{480} - \frac{13829\pi^2}{27648} - \frac{819703}{18432} \right) C_F^3 \right. \\
 & + C_A \left(-\frac{5l_2^4}{18} - \frac{109}{72} \pi^2 l_2^2 - \frac{711\pi^2 l_2}{32} - \frac{20a_4}{3} - \frac{105\pi^2 \zeta_3}{64} + \frac{16697\zeta_3}{768} + \frac{315\zeta_5}{64} + \frac{2261\pi^4}{8640} + \frac{83269\pi^2}{4608} - \frac{5891549}{55296} \right) C_F^2 \\
 & + C_A^2 \left(\frac{55l_2^4}{72} + \frac{77}{72} \pi^2 l_2^2 - \frac{67\pi^2 l_2}{4} + \frac{55a_4}{3} + \frac{29\pi^2 \zeta_3}{64} + \frac{6305\zeta_3}{288} - \frac{5\zeta_5}{16} - \frac{355\pi^4}{3456} + \frac{144577\pi^2}{13824} - \frac{2188757}{27648} \right) C_F \left. \right\} \frac{1}{\epsilon} \\
 & + \left\{ \left(-\frac{5497l_2^5}{960} - \frac{25}{32} \pi^2 l_2^4 + \frac{1113l_2^4}{16} - \frac{1753}{288} \pi^2 l_2^3 + \frac{49}{32} \pi^4 l_2^2 + \frac{3193}{24} \pi^2 l_2^2 - \frac{597}{32} \pi^2 \zeta_3 l_2 + \frac{47879\pi^4 l_2}{11520} \right. \right.
 \end{aligned}$$

$$\begin{aligned}
 & -\frac{580283\pi^2 l_2}{1536} + \frac{273\zeta_3^2}{128} + \frac{3339a_4}{2} + \frac{5497a_5}{8} - \frac{30763\pi^2 \zeta_3}{768} + \frac{702863\zeta_3}{1024} - \frac{263441\zeta_5}{512} + \frac{1349\pi^6}{7560} - \frac{50003\pi^4}{11520} \\
 & - \frac{75a_4\pi^2}{4} + \frac{954883\pi^2}{9216} + \frac{1233161}{12288} \Big) C_F^4 + C_A \left(-\frac{11719l_2^5}{1920} - \frac{41}{32}\pi^2 l_2^4 + \frac{7675l_2^4}{192} - \frac{11503}{576}\pi^2 l_2^3 + \frac{17}{32}\pi^4 l_2^2 + \frac{15679}{96}\pi^2 l_2^2 \right. \\
 & - \frac{789}{32}\pi^2 \zeta_3 l_2 + \frac{66053\pi^4 l_2}{23040} - \frac{168439\pi^2 l_2}{1024} + \frac{3937\zeta_3^2}{64} + \frac{7675a_4}{8} + \frac{11719a_5}{16} + \frac{1529\pi^2 \zeta_3}{384} + \frac{2917189\zeta_3}{6144} - \frac{895973\zeta_5}{1024} \\
 & + \frac{4763\pi^6}{10080} - \frac{10254293\pi^4}{737280} - \frac{123a_4\pi^2}{4} + \frac{7263359\pi^2}{73728} + \frac{518789}{2048} \Big) C_F^3 + C_A^2 \left(\frac{89l_2^5}{144} - \frac{97}{384}\pi^2 l_2^4 - \frac{43913l_2^4}{3456} \right. \\
 & - \frac{595}{432}\pi^2 l_2^3 + \frac{169}{384}\pi^4 l_2^2 - \frac{11153\pi^2 l_2^2}{1728} - \frac{751}{128}\pi^2 \zeta_3 l_2 - \frac{11185\pi^4 l_2}{6912} + \frac{169367\pi^2 l_2}{1728} + \frac{4813\zeta_3^2}{512} - \frac{43913a_4}{144} - \frac{445a_5}{6} \\
 & + \frac{179791\pi^2 \zeta_3}{9216} - \frac{12445\zeta_3}{9216} - \frac{24275\zeta_5}{1024} + \frac{19679\pi^6}{241920} - \frac{17671879\pi^4}{6635520} - \frac{97a_4\pi^2}{16} + \frac{5799935\pi^2}{221184} + \frac{92980613}{221184} \Big) C_F^2 \\
 & + n_l^3 T^3 \left(-\frac{3073\zeta_3}{648} - \frac{259\pi^4}{2160} - \frac{6035\pi^2}{5184} - \frac{620897}{93312} \right) C_F + n_h n_l^2 T^3 \left(\frac{5l_2^4}{9} + \frac{10}{9}\pi^2 l_2^2 - \frac{31\pi^2 l_2}{9} + \frac{40a_4}{3} + \frac{1319\zeta_3}{216} \right. \\
 & - \frac{289\pi^4}{2160} + \frac{11\pi^2}{576} - \frac{974489}{31104} \Big) C_F + n_h^3 T^3 \left(\frac{5l_2^4}{9} + \frac{4}{9}\pi^2 l_2^2 - \frac{83\pi^2 l_2}{45} + \frac{40a_4}{3} + \frac{34099\zeta_3}{3240} - \frac{167\pi^4}{2160} + \frac{220129\pi^2}{129600} \right. \\
 & - \frac{8242477}{466560} \Big) C_F + n_h^2 n_l T^3 \left(\frac{10l_2^4}{9} + \frac{14}{9}\pi^2 l_2^2 - \frac{238\pi^2 l_2}{45} + \frac{80a_4}{3} + \frac{23083\zeta_3}{1080} - \frac{197\pi^4}{2160} + \frac{124493\pi^2}{43200} - \frac{6585109}{155520} \right) C_F \\
 & + C_A^3 \left(\frac{2783l_2^5}{1440} + \frac{209}{384}\pi^2 l_2^4 - \frac{5329l_2^4}{432} + \frac{2783}{432}\pi^2 l_2^3 - \frac{209}{384}\pi^4 l_2^2 - \frac{23429}{432}\pi^2 l_2^2 + \frac{1463}{128}\pi^2 \zeta_3 l_2 - \frac{7381\pi^4 l_2}{17280} \right. \\
 & + \frac{67979\pi^2 l_2}{1728} - \frac{1507\zeta_3^2}{64} - \frac{5329a_4}{18} - \frac{2783a_5}{12} - \frac{187\pi^2 \zeta_3}{256} - \frac{3503635\zeta_3}{41472} + \frac{203005\zeta_5}{768} - \frac{104159\pi^6}{483840} + \frac{219365\pi^4}{41472} \\
 & + \frac{209a_4\pi^2}{16} + \frac{1818263\pi^2}{331776} + \frac{1829511217}{5971968} \Big) C_F + n_h^2 T^2 \left(\left(-\frac{l_2^5}{3} - \frac{443l_2^4}{108} - \frac{4}{9}\pi^2 l_2^3 - \frac{907}{108}\pi^2 l_2^2 + \frac{11\pi^4 l_2}{36} \right. \right. \\
 & + \frac{16829\pi^2 l_2}{540} - \frac{886a_4}{9} + 40a_5 - \frac{233\pi^2 \zeta_3}{48} - \frac{1643\zeta_3}{20} - \frac{385\zeta_5}{24} + \frac{317377\pi^4}{414720} - \frac{730669\pi^2}{38400} + \frac{52140391}{414720} \Big) C_F^2 \\
 & + C_A \left(\frac{l_2^5}{6} + \frac{1}{8}\pi^2 l_2^4 - \frac{233l_2^4}{27} + \frac{2}{9}\pi^2 l_2^3 - \frac{1}{8}\pi^4 l_2^2 - \frac{1613}{54}\pi^2 l_2^2 + \frac{21}{8}\pi^2 \zeta_3 l_2 - \frac{11\pi^4 l_2}{72} + \frac{27899\pi^2 l_2}{540} + \frac{19\zeta_3^2}{8} - \frac{1864a_4}{9} \right. \\
 & - 20a_5 + \frac{175\pi^2 \zeta_3}{48} - \frac{665293\zeta_3}{4320} + \frac{37\zeta_5}{48} - \frac{41\pi^6}{1080} + \frac{3851\pi^4}{3240} + 3a_4\pi^2 - \frac{18335563\pi^2}{1036800} + \frac{31646753}{207360} \Big) C_F \\
 & + n_l^2 T^2 \left(\left(-\frac{23l_2^5}{45} + \frac{89l_2^4}{27} - \frac{46}{27}\pi^2 l_2^3 + \frac{178}{27}\pi^2 l_2^2 + \frac{61\pi^4 l_2}{540} - \frac{355\pi^2 l_2}{27} + \frac{712a_4}{9} + \frac{184a_5}{3} - \frac{95\pi^2 \zeta_3}{48} + \frac{32747\zeta_3}{576} \right. \right. \\
 & - \frac{1657\zeta_5}{24} - \frac{78943\pi^4}{414720} + \frac{191657\pi^2}{13824} + \frac{735901}{13824} \Big) C_F^2 + C_A \left(\frac{23l_2^5}{90} - \frac{89l_2^4}{54} + \frac{23}{27}\pi^2 l_2^3 - \frac{89}{27}\pi^2 l_2^2 - \frac{61\pi^4 l_2}{1080} \right. \\
 & + \frac{355\pi^2 l_2}{54} - \frac{356a_4}{9} - \frac{92a_5}{3} + \frac{37\pi^2 \zeta_3}{48} + \frac{14887\zeta_3}{864} + \frac{1519\zeta_5}{48} + \frac{325\pi^4}{324} + \frac{298109\pi^2}{41472} + \frac{3159661}{41472} \Big) C_F \\
 & + n_h n_l T^2 \left(\left(-\frac{38l_2^5}{45} - \frac{31l_2^4}{72} - \frac{58}{27}\pi^2 l_2^3 - \frac{155}{36}\pi^2 l_2^2 + \frac{113\pi^4 l_2}{270} + \frac{191\pi^2 l_2}{8} - \frac{31a_4}{3} + \frac{304a_5}{3} - \frac{41\pi^2 \zeta_3}{6} - \frac{5293\zeta_3}{144} \right. \right. \\
 & - \frac{1021\zeta_5}{12} - \frac{20837\pi^4}{69120} - \frac{5063\pi^2}{864} + \frac{14881105}{82944} \Big) C_F^2 + C_A \left(\frac{19l_2^5}{45} + \frac{1}{8}\pi^2 l_2^4 - \frac{185l_2^4}{18} + \frac{29}{27}\pi^2 l_2^3 - \frac{1}{8}\pi^4 l_2^2 - 35\pi^2 l_2^2 \right.
 \end{aligned}$$

$$\begin{aligned}
 & + \frac{21}{8} \pi^2 \zeta_3 l_2 - \frac{113 \pi^4 l_2}{540} + \frac{2255 \pi^2 l_2}{36} + \frac{19 \zeta_3^2}{8} - \frac{740 a_4}{3} - \frac{152 a_5}{3} + \frac{53 \pi^2 \zeta_3}{12} - \frac{65105 \zeta_3}{432} + \frac{389 \zeta_5}{12} - \frac{41 \pi^6}{1080} + \frac{27 \pi^4}{16} \\
 & + 3 a_4 \pi^2 - \frac{254659 \pi^2}{20736} + \frac{4764781}{20736} \Big) C_F \Big) + n_h T \Big(\Big(\frac{57 l_2^5}{20} + \frac{1}{8} \pi^2 l_2^4 - \frac{2641 l_2^4}{256} + \frac{11}{4} \pi^2 l_2^3 - \frac{1}{8} \pi^4 l_2^2 - \frac{187}{128} \pi^2 l_2^2 \\
 & + \frac{21}{8} \pi^2 \zeta_3 l_2 - \frac{521 \pi^4 l_2}{160} + \frac{823 \pi^2 l_2}{256} - \frac{\zeta_3^2}{2} - \frac{7923 a_4}{32} - 342 a_5 + \frac{5743 \pi^2 \zeta_3}{192} - \frac{107213 \zeta_3}{4608} + \frac{6503 \zeta_5}{32} - \frac{5 \pi^6}{189} \\
 & + \frac{63667 \pi^4}{184320} + 3 a_4 \pi^2 + \frac{2023643 \pi^2}{165888} - \frac{26730911}{110592} \Big) C_F^3 + C_A \Big(\frac{37 l_2^5}{45} - \frac{19}{96} \pi^2 l_2^4 + \frac{12683 l_2^4}{384} + \frac{503}{108} \pi^2 l_2^3 + \frac{19}{96} \pi^4 l_2^2 \\
 & + \frac{127015 \pi^2 l_2^2}{1152} - \frac{133}{32} \pi^2 \zeta_3 l_2 + \frac{5041 \pi^4 l_2}{8640} - \frac{18911 \pi^2 l_2}{72} - \frac{3219 \zeta_3^2}{128} + \frac{12683 a_4}{16} - \frac{296 a_5}{3} - \frac{2437 \pi^2 \zeta_3}{256} + \frac{284675 \zeta_3}{512} \\
 & + \frac{134183 \zeta_5}{768} + \frac{7 \pi^6}{216} - \frac{103817 \pi^4}{55296} - \frac{19 a_4 \pi^2}{4} + \frac{5872135 \pi^2}{82944} - \frac{183814805}{331776} \Big) C_F^2 + C_A^2 \Big(-\frac{209 l_2^5}{180} - \frac{13}{24} \pi^2 l_2^4 + \frac{433 l_2^4}{18} \\
 & - \frac{319}{108} \pi^2 l_2^3 + \frac{13}{24} \pi^4 l_2^2 + \frac{1183}{12} \pi^2 l_2^2 - \frac{91}{8} \pi^2 \zeta_3 l_2 + \frac{1243 \pi^4 l_2}{2160} - \frac{10241 \pi^2 l_2}{72} + \frac{65 \zeta_3^2}{32} + \frac{1732 a_4}{3} + \frac{418 a_5}{3} - \frac{937 \pi^2 \zeta_3}{96} \\
 & + \frac{430415 \zeta_3}{1152} - \frac{9431 \zeta_5}{96} + \frac{22097 \pi^6}{120960} - \frac{53237 \pi^4}{11520} - 13 a_4 \pi^2 + \frac{347143 \pi^2}{10368} - \frac{197507311}{497664} \Big) C_F \Big) \\
 & + n_l T \Big(\Big(\frac{383 l_2^5}{120} + \frac{1}{8} \pi^2 l_2^4 - \frac{685 l_2^4}{24} + \frac{275}{36} \pi^2 l_2^3 - \frac{1}{8} \pi^4 l_2^2 - \frac{166}{3} \pi^2 l_2^2 + \frac{21}{8} \pi^2 \zeta_3 l_2 - \frac{257 \pi^4 l_2}{180} + \frac{579 \pi^2 l_2}{4} - \frac{\zeta_3^2}{2} \\
 & - 685 a_4 - 383 a_5 + \frac{3169 \pi^2 \zeta_3}{192} - \frac{245419 \zeta_3}{768} + \frac{23615 \zeta_5}{64} - \frac{5 \pi^6}{189} + \frac{484063 \pi^4}{184320} + 3 a_4 \pi^2 - \frac{1185613 \pi^2}{18432} - \frac{152405}{1024} \Big) C_F^3 \\
 & + C_A \Big(\frac{175 l_2^5}{144} + \frac{1}{3} \pi^2 l_2^4 - \frac{1661 l_2^4}{432} + \frac{1199}{216} \pi^2 l_2^3 - \frac{1}{3} \pi^4 l_2^2 - \frac{3247}{108} \pi^2 l_2^2 + 7 \pi^2 \zeta_3 l_2 + \frac{5 \pi^4 l_2}{54} - \frac{385 \pi^2 l_2}{54} - \frac{249 \zeta_3^2}{16} \\
 & - \frac{1661 a_4}{18} - \frac{875 a_5}{6} - \frac{1763 \pi^2 \zeta_3}{384} - \frac{87917 \zeta_3}{576} + \frac{85783 \zeta_5}{384} - \frac{7709 \pi^6}{60480} + \frac{2344277 \pi^4}{829440} + 8 a_4 \pi^2 - \frac{643145 \pi^2}{13824} - \frac{151453}{512} \Big) C_F^2 \\
 & + C_A^2 \Big(-\frac{253 l_2^5}{180} - \frac{19}{96} \pi^2 l_2^4 + \frac{3913 l_2^4}{432} - \frac{253}{54} \pi^2 l_2^3 + \frac{19}{96} \pi^4 l_2^2 + \frac{6235}{216} \pi^2 l_2^2 - \frac{133}{32} \pi^2 \zeta_3 l_2 + \frac{671 \pi^4 l_2}{2160} - \frac{14093 \pi^2 l_2}{432} \\
 & + \frac{137 \zeta_3^2}{16} + \frac{3913 a_4}{18} + \frac{506 a_5}{3} - \frac{89 \pi^2 \zeta_3}{48} + \frac{23219 \zeta_3}{1152} - \frac{8791 \zeta_5}{48} + \frac{9469 \pi^6}{120960} - \frac{392849 \pi^4}{103680} - \frac{19 a_4 \pi^2}{4} \\
 & - \frac{264949 \pi^2}{20736} - \frac{134979991}{497664} \Big) C_F \Big) \Big\} + \xi \Big[\left\{ T n_h \left(\frac{1}{256} C_A C_F^2 - \frac{9 C_F^3}{128} \right) + \frac{477 C_A C_F^3}{2048} - \frac{9}{128} T C_F^3 n_l + \frac{297 C_F^4}{512} \right\} \frac{1}{\epsilon^4} \right. \\
 & + \left\{ T n_h \left(-\frac{5}{768} C_A C_F^2 - \frac{75 C_F^3}{256} \right) + \left(\frac{2271}{2048} - \frac{3 \pi^2}{512} \right) C_A C_F^3 - \frac{75}{256} T C_F^3 n_l + \frac{999 C_F^4}{1024} \right\} \frac{1}{\epsilon^3} \\
 & + \left\{ \left(\frac{9 \zeta_3}{1024} - \frac{\pi^4}{5760} + \frac{1}{1024} \right) C_A^2 C_F^2 + T n_h \left(\left(\frac{31}{768} + \frac{\pi^2}{768} \right) C_A C_F^2 + \left(\frac{9 \pi^2}{128} - \frac{913}{512} \right) C_F^3 \right) \right. \\
 & + C_A C_F^3 \left(-\frac{9 \zeta_3}{32} + \frac{9 \pi^2 l_2}{64} + \frac{37 \pi^2}{2048} + \frac{1387}{256} \right) + C_F^4 \left(\frac{27 \zeta_3}{64} - \frac{9}{32} \pi^2 l_2 + \frac{225 \pi^2}{512} + \frac{12069}{2048} \right) \\
 & + \left(-\frac{697}{512} - \frac{9 \pi^2}{128} \right) T C_F^3 n_l \Big\} \frac{1}{\epsilon^2} + \left\{ C_A C_F^3 \left(-\frac{27 a_4}{8} - \frac{1245 \zeta_3}{512} - \frac{9 l_2^4}{64} - \frac{9}{32} \pi^2 l_2^2 + \frac{15 \pi^2 l_2}{16} + \frac{21 \pi^4}{512} + \frac{377 \pi^2}{6144} \right. \right. \\
 & \left. \left. + \frac{80197}{4096} \right) + C_F^4 \left(\frac{27 a_4}{4} + \frac{639 \zeta_3}{128} + \frac{9 l_2^4}{32} + \frac{9}{16} \pi^2 l_2^2 - \frac{15 \pi^2 l_2}{8} - \frac{63 \pi^4}{640} + \frac{1659 \pi^2}{1024} + \frac{49519}{4096} \right) \right.
 \end{aligned}$$

$$\begin{aligned}
 & + \left(-\frac{1}{192}\pi^2\zeta_3 + \frac{51\zeta_3}{1024} - \frac{7\zeta_5}{512} - \frac{383\pi^4}{552960} + \frac{3\pi^2}{1024} + \frac{43}{3072} \right) C_A^2 C_F^2 + Tn_h \left(\left(\frac{5\zeta_3}{192} - \frac{5\pi^2}{2304} - \frac{97}{768} \right) C_A C_F^2 \right. \\
 & + C_F^3 \left(\frac{33\zeta_3}{16} - \frac{9}{16}\pi^2 l_2 + \frac{111\pi^2}{256} - \frac{6899}{1024} \right) + \left. \left(-\frac{15\zeta_3}{32} - \frac{75\pi^2}{256} - \frac{4955}{1024} \right) T C_F^3 n_l \right) \frac{1}{\epsilon} \\
 & + Tn_h \left(C_F^3 \left(\frac{27a_4}{2} + \frac{739\zeta_3}{64} + \frac{9l_2^4}{16} + \frac{9}{8}\pi^2 l_2^2 - \frac{51\pi^2 l_2}{16} - \frac{9\pi^4}{128} + \frac{997\pi^2}{512} - \frac{54873}{2048} \right) \right. \\
 & + \left. \left(-\frac{25\zeta_3}{576} - \frac{\pi^4}{768} + \frac{31\pi^2}{2304} + \frac{1309}{2304} \right) C_A C_F^2 \right) + C_A C_F^3 \left(-\frac{45a_4}{2} - \frac{81a_5}{4} + \frac{37\pi^2\zeta_3}{128} - \frac{6083\zeta_3}{512} + \frac{5157\zeta_5}{256} \right. \\
 & + \left. \frac{27l_2^5}{160} - \frac{15l_2^4}{16} + \frac{9}{16}\pi^2 l_2^3 - \frac{15}{8}\pi^2 l_2^2 - \frac{63\pi^4 l_2}{640} + \frac{143\pi^2 l_2}{32} + \frac{533\pi^4}{2048} + \frac{2297\pi^2}{3072} + \frac{609965}{8192} \right) \\
 & + C_F^4 \left(45a_4 + \frac{81a_5}{2} - \frac{45\pi^2\zeta_3}{64} + \frac{7077\zeta_3}{256} - \frac{5481\zeta_5}{128} - \frac{27l_2^5}{80} + \frac{15l_2^4}{8} - \frac{9}{8}\pi^2 l_2^3 + \frac{15}{4}\pi^2 l_2^2 + \frac{63\pi^4 l_2}{320} - \frac{143\pi^2 l_2}{16} \right. \\
 & - \left. \frac{699\pi^4}{2560} + \frac{17449\pi^2}{2048} + \frac{433933}{8192} \right) + \left(-\frac{25\zeta_3^2}{512} - \frac{115\pi^2\zeta_3}{9216} + \frac{265\zeta_3}{1024} + \frac{391\zeta_5}{3072} - \frac{5\pi^6}{6912} - \frac{349\pi^4}{110592} \right. \\
 & + \left. \frac{91\pi^2}{3072} + \frac{125}{1024} \right) C_A^2 C_F^2 + \left(-\frac{125\zeta_3}{64} - \frac{9\pi^4}{128} - \frac{697\pi^2}{512} - \frac{35505}{2048} \right) T C_F^3 n_l + \xi^2 \left[\left\{ \frac{27C_F^4}{1024} - \frac{27C_A C_F^3}{2048} \right\} \frac{1}{\epsilon^4} \right. \\
 & + \left. \left\{ \frac{27C_F^4}{512} - \frac{135C_A C_F^3}{4096} \right\} \frac{1}{\epsilon^3} + \left\{ \left(-\frac{1071}{4096} - \frac{27\pi^2}{2048} \right) C_A C_F^3 + \left(\frac{117}{256} + \frac{27\pi^2}{1024} \right) C_F^4 \right\} \frac{1}{\epsilon^2} \right. \\
 & + \left. \left\{ \left(-\frac{45\zeta_3}{512} - \frac{135\pi^2}{4096} - \frac{2117}{4096} \right) C_A C_F^3 + \left(\frac{45\zeta_3}{256} + \frac{27\pi^2}{512} + \frac{169}{256} \right) C_F^4 \right\} \frac{1}{\epsilon} + \left(-\frac{225\zeta_3}{1024} - \frac{27\pi^4}{2048} \right. \right. \\
 & \left. \left. - \frac{1071\pi^2}{4096} - \frac{14895}{4096} \right) C_A C_F^3 + \left(\frac{45\zeta_3}{128} + \frac{27\pi^4}{1024} + \frac{117\pi^2}{256} + \frac{1531}{256} \right) C_F^4 \right], \tag{D3}
 \end{aligned}$$

where a_n and l_2 are given in Eqs. (39) and (C5), respectively. The QCD gauge parameter ξ is defined via the gluon propagator

$$D_g^{\mu\nu}(q) = -i \frac{g^{\mu\nu} - \xi \frac{q^\mu q^\nu}{q^2}}{q^2 + i\epsilon}. \tag{D4}$$

APPENDIX E: ANALYTIC RESULTS FOR z_m

In this appendix we repeat for convenience the coefficients of the color structures presented in Sec. III C which are known analytically [67]. They are given by

$$\begin{aligned}
 Z_m^{FLLL} &= \frac{317\zeta_3}{432} + \frac{71\pi^4}{4320} + \frac{89\pi^2}{648} + \frac{42979}{186624}, & Z_m^{FLLH} &= \frac{5\zeta_3}{144} - \frac{19\pi^4}{480} + \frac{\pi^2}{6} + \frac{128515}{62208}, \\
 Z_m^{FFLL} &= \frac{2l_2^5}{45} - \frac{11l_2^4}{27} + \frac{4}{27}\pi^2 l_2^3 - \frac{22}{27}\pi^2 l_2^2 + \frac{31}{540}\pi^4 l_2 + \frac{103}{54}\pi^2 l_2 - \frac{88a_4}{9} - \frac{16a_5}{3} + \frac{305\zeta_3}{48} + \frac{3\pi^2\zeta_3}{8} - \frac{2839\zeta_3}{576} + \frac{3683\pi^4}{51840} \\
 & - \frac{5309\pi^2}{3456} - \frac{2396921}{497664}, \\
 Z_m^{FALL} &= -\frac{1}{45}l_2^5 + \frac{11l_2^4}{54} - \frac{2}{27}\pi^2 l_2^3 + \frac{11}{27}\pi^2 l_2^2 - \frac{31\pi^4 l_2}{1080} - \frac{103}{108}\pi^2 l_2 + \frac{44a_4}{9} + \frac{8a_5}{3} - \frac{41\zeta_3}{24} - \frac{13\pi^2\zeta_3}{48} - \frac{3245\zeta_3}{576} - \frac{4723\pi^4}{51840} \\
 & - \frac{527\pi^2}{384} - \frac{2708353}{497664}, \tag{E1}
 \end{aligned}$$

where a_n and l_2 are given in Eqs. (39) and (C5), respectively.

APPENDIX F: $Z_m^{\overline{\text{MS}}}$ FOR GENERAL $\text{SU}(N_c)$ GAUGE GROUP

In this appendix we present $Z_m^{\overline{\text{MS}}}$ up to four-loop order [24,25] expressed in terms of $\text{SU}(N_c)$ color factors. It has been obtained from the quark mass anomalous dimension given in [25].

$$\begin{aligned}
Z_m^{\overline{\text{MS}}} = & 1 - \frac{3C_F \alpha_s}{4\epsilon \pi} + \left\{ \left[\frac{9C_F^2}{32} + \frac{11C_A C_F}{32} - \frac{1}{8} n_f T C_F \right] \frac{1}{\epsilon^2} + \left[-\frac{3C_F^2}{64} - \frac{97C_A C_F}{192} + \frac{5}{48} n_f T C_F \right] \frac{1}{\epsilon} \right\} \left(\frac{\alpha_s}{\pi} \right)^2 \\
& + \left\{ \left[-\frac{9C_F^3}{128} - \frac{33}{128} C_A C_F^2 - \frac{121}{576} C_A^2 C_F - \frac{1}{36} n_f^2 T^2 C_F + \left(\frac{3C_F^2}{32} + \frac{11C_A C_F}{72} \right) n_f T \right] \frac{1}{\epsilon^3} \right. \\
& + \left[\frac{9C_F^3}{256} + \frac{313}{768} C_A C_F^2 + \frac{1679C_A^2 C_F}{3456} + \frac{5}{216} n_f^2 T^2 C_F + \left(-\frac{29C_F^2}{192} - \frac{121C_A C_F}{432} \right) n_f T \right] \frac{1}{\epsilon^2} \\
& + \left[-\frac{43C_F^3}{128} + \frac{43}{256} C_A C_F^2 - \frac{11413C_A^2 C_F}{20736} + \frac{35n_f^2 T^2 C_F}{1296} \right. \\
& + \left. n_f T \left(\left(\frac{23}{96} - \frac{\zeta_3}{4} \right) C_F^2 + C_A \left(\frac{\zeta_3}{4} + \frac{139}{1296} \right) C_F \right) \right] \frac{1}{\epsilon} \left\} \left(\frac{\alpha_s}{\pi} \right)^3 \\
& + \left\{ \left[\frac{27C_F^4}{2048} + \frac{99C_A C_F^3}{1024} + \frac{1331C_A^2 C_F^2}{6144} + \frac{1331C_A^3 C_F}{9216} - \frac{1}{144} n_f^3 T^3 C_F \right. \right. \\
& + \left. \left(\frac{11C_F^2}{384} + \frac{11C_A C_F}{192} \right) n_f^2 T^2 + \left(-\frac{9C_F^3}{256} - \frac{121}{768} C_A C_F^2 - \frac{121}{768} C_A^2 C_F \right) n_f T \right] \frac{1}{\epsilon^4} \\
& + \left[-\frac{27C_F^4}{2048} - \frac{23}{128} C_A C_F^3 - \frac{1285C_A^2 C_F^2}{2304} - \frac{25201C_A^3 C_F}{55296} + \frac{5}{864} n_f^3 T^3 C_F \right. \\
& + \left. \left(-\frac{37C_F^2}{576} - \frac{43C_A C_F}{384} \right) n_f^2 T^2 + \left(\frac{23C_F^3}{256} + \frac{943C_A C_F^2}{2304} + \frac{1981C_A^2 C_F}{4608} \right) n_f T \right] \frac{1}{\epsilon^3} \\
& + \left[\frac{2073C_F^4}{8192} + \frac{527C_A C_F^3}{4096} + \frac{97661C_A^2 C_F^2}{221184} + \frac{236333C_A^3 C_F}{331776} + \frac{35n_f^3 T^3 C_F}{5184} \right. \\
& + \left. n_f^2 T^2 \left(\left(\frac{1001}{13824} - \frac{\zeta_3}{16} \right) C_F^2 + C_A \left(\frac{\zeta_3}{16} + \frac{217}{4608} \right) C_F \right) + n_f T \left(\left(\frac{3\zeta_3}{16} - \frac{275}{1024} \right) C_F^3 \right. \right. \\
& + \left. \left. C_A \left(-\frac{\zeta_3}{64} - \frac{10933}{27648} \right) C_F^2 + C_A^2 \left(-\frac{11\zeta_3}{64} - \frac{7009}{13824} \right) C_F \right) \right] \frac{1}{\epsilon^2} \\
& + \left[\left(\frac{21\zeta_3}{64} + \frac{1261}{8192} \right) C_F^4 + C_A \left(-\frac{79\zeta_3}{256} - \frac{15349}{12288} \right) C_F^3 + C_A^2 \left(\frac{19\zeta_3}{128} - \frac{55\zeta_5}{128} + \frac{34045}{36864} \right) C_F^2 \right. \\
& + \left. n_f^3 T^3 \left(\frac{83}{10368} - \frac{\zeta_3}{72} \right) C_F + C_A^3 \left(-\frac{709\zeta_3}{4608} + \frac{55\zeta_5}{128} - \frac{70055}{73728} \right) C_F \right. \\
& + \left. n_f^2 T^2 \left(\left(\frac{5\zeta_3}{32} - \frac{\pi^4}{960} - \frac{19}{1728} \right) C_F^2 + C_A \left(-\frac{5\zeta_3}{32} + \frac{\pi^4}{960} - \frac{671}{41472} \right) C_F \right) \right. \\
& + \left. \frac{d_{FA}}{N_c} \left(\frac{1}{32} - \frac{15\zeta_3}{64} \right) + n_f \left(\frac{d_{FF}}{N_c} \left(\frac{15\zeta_3}{32} - \frac{1}{16} \right) + T \left(\left(-\frac{69\zeta_3}{128} + \frac{15\zeta_5}{32} + \frac{35}{384} \right) C_F^3 \right. \right. \right. \\
& + \left. \left. C_A \left(-\frac{23\zeta_3}{64} - \frac{5\zeta_5}{64} + \frac{11\pi^4}{3840} + \frac{8819}{27648} \right) C_F^2 \right. \right. \\
& + \left. \left. C_A^2 \left(\frac{671\zeta_3}{768} - \frac{25\zeta_5}{64} - \frac{11\pi^4}{3840} + \frac{65459}{165888} \right) C_F \right) \right] \frac{1}{\epsilon} \left\} \left(\frac{\alpha_s}{\pi} \right)^4, \tag{F1}
\end{aligned}$$

where d_{FF} and d_{FA} are defined in Eq. (C5).

- [1] P. Nason, *Proc. Sci.*, TOP2015 (2016) 056 [arXiv:1602.00443].
- [2] M. Beneke, P. Marquard, P. Nason, and M. Steinhauser, arXiv:1605.03609.
- [3] K. G. Chetyrkin, J. H. Kuhn, A. Maier, P. Maierhofer, P. Marquard, M. Steinhauser, and C. Sturm, *Phys. Rev. D* **80**, 074010 (2009).
- [4] M. Beneke, *Phys. Lett. B* **434**, 115 (1998).
- [5] A. H. Hoang, Z. Ligeti, and A. V. Manohar, *Phys. Rev. D* **59**, 074017 (1999).
- [6] A. H. Hoang, Z. Ligeti, and A. V. Manohar, *Phys. Rev. Lett.* **82**, 277 (1999).
- [7] A. H. Hoang and T. Teubner, *Phys. Rev. D* **60**, 114027 (1999).
- [8] A. Pineda, *J. High Energy Phys.* 06 (2001) 022.
- [9] A. Czarnecki, K. Melnikov, and N. Uraltsev, *Phys. Rev. Lett.* **80**, 3189 (1998).
- [10] ATLAS and CDF and CMS and D0 Collaborations, arXiv:1403.4427.
- [11] P. Z. Skands and D. Wicke, *Eur. Phys. J. C* **52**, 133 (2007).
- [12] S. Kawabata, Y. Shimizu, Y. Sumino, and H. Yokoya, *Phys. Lett. B* **741**, 232 (2015).
- [13] J. Kieseler, K. Lipka, and S. O. Moch, *Phys. Rev. Lett.* **116**, 162001 (2016).
- [14] M. Beneke, Y. Kiyo, P. Marquard, A. Penin, J. Piclum, and M. Steinhauser, *Phys. Rev. Lett.* **115**, 192001 (2015).
- [15] F. Simon, arXiv:1603.04764.
- [16] Y. Kiyo, G. Mishima, and Y. Sumino, *J. High Energy Phys.* 11 (2015) 084.
- [17] A. A. Penin and N. Zerf, *J. High Energy Phys.* 04 (2014) 120.
- [18] M. Beneke, A. Maier, J. Piclum, and T. Rauh, *Nucl. Phys. B* **891**, 42 (2015).
- [19] A. A. Penin and M. Steinhauser, *Phys. Lett. B* **538**, 335 (2002).
- [20] C. Ayala, G. Cvetič, and A. Pineda, *J. High Energy Phys.* 09 (2014) 045.
- [21] Y. Kiyo, G. Mishima, and Y. Sumino, *Phys. Lett. B* **752**, 122 (2016).
- [22] C. Ayala, G. Cvetič, and A. Pineda, arXiv:1606.01741.
- [23] P. A. Baikov, K. G. Chetyrkin, and J. H. Kühn, *J. High Energy Phys.* 10 (2014) 76.
- [24] K. G. Chetyrkin, *Phys. Lett. B* **404**, 161 (1997).
- [25] J. A. M. Vermaseren, S. A. Larin, and T. van Ritbergen, *Phys. Lett. B* **405**, 327 (1997).
- [26] K. G. Chetyrkin, *Nucl. Phys. B* **710**, 499 (2005).
- [27] T. van Ritbergen, A. N. Schellekens, and J. A. M. Vermaseren, *Int. J. Mod. Phys. A* **14**, 41 (1999).
- [28] R. Tarrach, *Nucl. Phys. B* **183**, 384 (1981).
- [29] N. Gray, D. J. Broadhurst, W. Grafe, and K. Schilcher, *Z. Phys. C* **48**, 673 (1990).
- [30] K. G. Chetyrkin and M. Steinhauser, *Phys. Rev. Lett.* **83**, 4001 (1999).
- [31] K. G. Chetyrkin and M. Steinhauser, *Nucl. Phys. B* **573**, 617 (2000).
- [32] K. Melnikov and T. v. Ritbergen, *Phys. Lett. B* **482**, 99 (2000).
- [33] P. Marquard, L. Mihaila, J. H. Piclum, and M. Steinhauser, *Nucl. Phys. B* **773**, 1 (2007).
- [34] R. Hempfling and B. A. Kniehl, *Phys. Rev. D* **51**, 1386 (1995).
- [35] F. Jegerlehner, M. Y. Kalmykov, and O. Veretin, *Nucl. Phys. B* **658**, 49 (2003).
- [36] F. Jegerlehner and M. Y. Kalmykov, *Nucl. Phys. B* **676**, 365 (2004).
- [37] F. Jegerlehner and M. Y. Kalmykov, *Acta Phys. Pol. B* **34**, 5335 (2003).
- [38] M. Faisst, J. H. Kühn, and O. Veretin, *Phys. Lett. B* **589**, 35 (2004).
- [39] S. P. Martin, *Phys. Rev. D* **72**, 096008 (2005).
- [40] D. Eiras and M. Steinhauser, *J. High Energy Phys.* 02 (2006) 010.
- [41] F. Jegerlehner, M. Y. Kalmykov, and B. A. Kniehl, *Phys. Lett. B* **722**, 123 (2013).
- [42] B. A. Kniehl, A. F. Pikelner, and O. L. Veretin, *Nucl. Phys. B* **896**, 19 (2015).
- [43] S. P. Martin, *Phys. Rev. D* **93**, 094017 (2016).
- [44] P. Marquard, A. V. Smirnov, V. A. Smirnov, and M. Steinhauser, *Phys. Rev. Lett.* **114**, 142002 (2015).
- [45] S. Bekavac, A. Grozin, D. Seidel, and M. Steinhauser, *J. High Energy Phys.* 10 (2007) 006.
- [46] K. G. Chetyrkin, J. H. Kühn, and M. Steinhauser, *Comput. Phys. Commun.* **133**, 43 (2000).
- [47] B. Schmidt and M. Steinhauser, *Comput. Phys. Commun.* **183**, 1845 (2012).
- [48] P. Nogueira, *J. Comput. Phys.* **105**, 279 (1993).
- [49] R. Harlander, T. Seidensticker, and M. Steinhauser, *Phys. Lett. B* **426**, 125 (1998).
- [50] T. Seidensticker, arXiv:hep-ph/9905298.
- [51] J. A. M. Vermaseren, arXiv:math-ph/0010025.
- [52] J. Kuipers, T. Ueda, J. A. M. Vermaseren, and J. Vollinga, *Comput. Phys. Commun.* **184**, 1453 (2013).
- [53] K. G. Chetyrkin and F. V. Tkachov, *Nucl. Phys. B* **192**, 159 (1981).
- [54] S. Laporta, *Int. J. Mod. Phys. A* **15**, 5087 (2000).
- [55] A. V. Smirnov, *J. High Energy Phys.* 10 (2008) 107.
- [56] A. V. Smirnov and V. A. Smirnov, *Comput. Phys. Commun.* **184**, 2820 (2013).
- [57] A. V. Smirnov, *Comput. Phys. Commun.* **189**, 182 (2015).
- [58] P. Marquard and D. Seidel (to be published).
- [59] R. N. Lee and A. A. Pomeransky, *J. High Energy Phys.* 11 (2013) 165.
- [60] A. V. Smirnov and M. N. Tentyukov, *Comput. Phys. Commun.* **180**, 735 (2009).
- [61] A. V. Smirnov, V. A. Smirnov, and M. Tentyukov, *Comput. Phys. Commun.* **182**, 790 (2011).
- [62] A. V. Smirnov, *Comput. Phys. Commun.* **185**, 2090 (2014).
- [63] T. Hahn, *Comput. Phys. Commun.* **168**, 78 (2005).
- [64] G. P. Lepage, Report No. CLNS-80/447.
- [65] A. von Manteuffel, E. Panzer, and R. M. Schabinger, *J. High Energy Phys.* 02 (2015) 120.
- [66] R. N. Lee and V. A. Smirnov, *J. High Energy Phys.* 02 (2011) 102.
- [67] R. Lee, P. Marquard, A. V. Smirnov, V. A. Smirnov, and M. Steinhauser, *J. High Energy Phys.* 03 (2013) 162.
- [68] M. Czakon, *Comput. Phys. Commun.* **175**, 559 (2006).

- [69] A. V. Smirnov and V. A. Smirnov, *Eur. Phys. J. C* **62**, 445 (2009).
- [70] D. Wellmann, Master thesis, KIT (unpublished).
- [71] T. Banks and A. Zaks, *Nucl. Phys.* **B196**, 189 (1982).
- [72] M. Beneke and V. M. Braun, *Phys. Lett. B* **348**, 513 (1995).
- [73] See Supplemental Material at <http://link.aps.org/supplemental/10.1103/PhysRevD.94.074025> for the formulas of Sec. IV D and the ones of the appendixes (except Appendix E) in computer readable format.
- [74] Y. Schroder and M. Steinhauser, *J. High Energy Phys.* **01** (2006) 051.
- [75] K. G. Chetyrkin, J. H. Kuhn, and C. Sturm, *Nucl. Phys.* **B744**, 121 (2006).
- [76] K. G. Chetyrkin, B. A. Kniehl, and M. Steinhauser, *Nucl. Phys.* **B510**, 61 (1998).
- [77] V. Sadovnichy, A. Tikhonravov, V. Voevodin, and V. Opanasenko, in *Contemporary High Performance Computing: From Petascale toward Exascale*, Chapman & Hall/CRC Computational Science (CRC Press, Boca Raton, 2013), pp. 283–307.
- [78] A. L. Kataev and V. S. Molokoedov, *Eur. Phys. J.* **131**, 271 (2016).